NAVAL POSTGRADUATE SCHOOL
MONTEREY, CALIFORNIA

THESIS

FAULT ASSESSMENT OF A DIESEL ENGINE USING VIBRATION MEASUREMENTS AND ADVANCED SIGNAL PROCESSING

by

Robert A. Armstrong

December 1996

Thesis Advisor: Knox T. Millsaps, Jr.

Approved for public release; distribution is unlimited.

DTIC QUALITY INSPECTED 1

DISCLAIMER NOTICE

THIS DOCUMENT IS BEST QUALITY AVAILABLE. THE COPY FURNISHED TO DTIC CONTAINED A SIGNIFICANT NUMBER OF COLOR PAGES WHICH DO NOT REPRODUCE LEGIBLY ON BLACK AND WHITE MICROFICHE.

REPORT DOCUMENTATION PAGE

Form Approved OMB No. 0704-0188

1. AGENCY USE ONLY *(Leave blank)*	2. REPORT DATE December 1996	3. REPORT TYPE AND DATES COVERED Engineer's Thesis

4. TITLE AND SUBTITLE FAULT ASSESSMENT OF A DIESEL ENGINE USING VIBRATION MEASUREMENTS AND ADVANCED SIGNAL PROCESSING	5. FUNDING NUMBERS
6. AUTHOR(S) Robert A. Armstrong	

7. PERFORMING ORGANIZATION NAME(S) AND ADDRESS(ES) Naval Postgraduate School Monterey CA 93943-5000	8. PERFORMING ORGANIZATION REPORT NUMBER

9. SPONSORING/MONITORING AGENCY NAME(S) AND ADDRESS(ES)	10. SPONSORING/MONITORING AGENCY REPORT NUMBER

11. SUPPLEMENTARY NOTES The views expressed in this thesis are those of the author and do not reflect the official policy or position of the Department of Defense or the U.S. Government.

12a. DISTRIBUTION/AVAILABILITY STATEMENT Approved for public release; distribution is unlimited.	12b. DISTRIBUTION CODE

13. ABSTRACT *(maximum 200 words)*

* A Diesel Engine test cell was developed, which consisted of a Detroit Diesel 3-53 engine, a water brake dynamometer and an engine cycle analyzer. Extensive steady state and time resolved instrumentation were installed along with a highspeed data acquisition system to obtain cylinder pressure and engine vibration data. High frequency response accelerometers were mounted on the cylinder head assembly to measure phase resolved response relative to top dead center (TDC) on the first cylinder. Baseline vibration data were taken over a range of engine load and speed combinations. An engine fault was introduced by adjusting the timing on the first cylinder injector. The vibration signatures of the baseline engine and the induced fault engine were characterized using Joint Time Frequency Analysis. The fault condition was detected and localized.

14. SUBJECT TERMS Joint Time Frequency Analysis, Engine Diagnosis, Reciprocating Machinery	15. NUMBER OF PAGES 77
	16. PRICE CODE

17. SECURITY CLASSIFICATION OF REPORT Unclassified	18. SECURITY CLASSIFICATION OF THIS PAGE Unclassified	19. SECURITY CLASSIFICATION OF ABSTRACT Unclassified	20. LIMITATION OF ABSTRACT UL

NSN 7540-01-280-5500

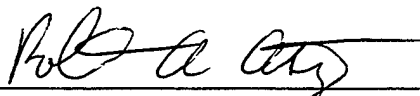Standard Form 298 (Rev. 2-89)
Prescribed by ANSI Std. 239-18 298-102

FAULT ASSESSMENT OF A DIESEL ENGINE USING VIBRATION MEASUREMENTS AND ADVANCED SIGNAL PROCESSING

Robert A. Armstrong

Lieutenant, United States Navy

B.S., University of Missouri, 1987

Submitted in partial fulfillment
of the requirements for the degree of

MASTER OF SCIENCE IN MECHANICAL ENGINEERING
and
MECHANICAL ENGINEER
from the
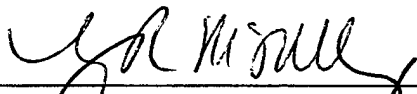**NAVAL POSTGRADUATE SCHOOL**
December 1996

Author: _____

Robert A. Armstrong

Approved by: _____

Knox T. Millsaps, Jr., Advisor

_____

Terry R. McNelley, Chairman
Department of Mechanical Engineering

iii

iv

ABSTRACT

A Diesel Engine test cell was developed, which consisted of a Detroit Diesel 3-53 engine, a water brake dynamometer and an engine cycle analyzer. Extensive steady state and time resolved instrumentation were installed along with a high speed data acquisition system to obtain cylinder pressure and engine vibration data. High frequency response accelerometers were mounted on the cylinder head assembly to measure phase resolved response relative to top dead center (TDC) on the first cylinder. Baseline vibration data were taken over a range of engine load and speed combinations. An engine fault was introduced by adjusting the timing on the first cylinder injector. The vibration signatures of the baseline engine and the induced fault engine were characterized using Joint Time Frequency Analysis. The fault condition was detected and localized.

TABLE OF CONTENTS

LIST OF FIGURES

LIST OF ABBREVIATIONS

A/D	Analog to Digital
ASD	Adaptive Spectrogram Distribution
bhp	Brake Horsepower
CBM	Condition Based Maintenance
CSD	Cone Shaped Distribution
CTI	Cross Term Interference
CWD	Choi-Williams Distribution
DETA	Diesel Engine Trend Analysis
DEUCE	Diesel Engine Unit Condition Evaluator
ECA	Engine Cycle Analyzer
ft lbs	Footpounds
hp	Horsepower
ICAS	Integrated Condition Assessment System
JTFA	Joint Time Frequency Analysis
JTFD	Joint Time Frequency Distribution
khz	Kilohertz
Mhz	Megahertz
psi	Pounds per square inch
rpm	Revolutions per minute
sec	Seconds
SEMMSS	Systems and Equipment Maintenance Monitoring for Surface Ships
STFT	Short Time Fourier Transform
TDC	Top Dead Center
WVD	Wigner-Ville Distribution

NOMENCLATURE

e	Exponential function
$h(\tau\text{-}t)$	Windowing function centered at time t
j	Imaginary number $\sqrt{-1}$
π	Pi constant
P(t)	Dynamic pressure loading in the cylinder with respect to time
$P_S(t,\omega)$	Energy density spectrum of the time domain signal
S^*	Conjugate of the time domain signal
$S(t)$	Time domain signal
$S_t(\omega)$	Fourier Transform of the time domain signal
t	Center point of the time window
τ	Integration variable
ω	Frequency
$WVD(t,\omega)$	Wigner-Ville Distribution of the time domain signal

I. INTRODUCTION

A. IMPORTANCE OF DIESEL ENGINES AND MAINTENANCE

Diesel engines can be found throughout the U.S. Navy surface and submarine fleets. They are utilized in propulsion and electric plants. The advantage of the Diesel engine is good fuel efficiency across its operating range. The acquisition cost is about the same as gas turbine engines in the 1,000-3,000 horsepower (hp) class. However, in the Navy's experience, maintenance on these engines is very expensive. Maintenance costs are nearly 3 times that of a gas turbine per horsepower-hour of operation. Diesel engines are overhauled on a periodic basis. The overhauls are performed in place onboard the ship resulting in a loss of operating time. The new trend is to shift all equipment to Condition Based Maintenance (CBM). This would reduce maintenance cost while increasing operational availability. For CBM to be effective, methods must be developed to monitor the health of the engine without interfering with normal operation. When an engine problem is detected the location must be isolated and the severity determined without performing extensive and costly teardowns of the engine.

Currently there is extensive research into the application of CBM for Diesel engines and reciprocating machinery. Methods are being developed to monitor operating efficiency and mechanical condition. The principle tools used are time domain signal analysis and frequency-spectra analysis of various engine signals. The advanced signal processing technique of Joint Time Frequency Analysis (JTFA) has been applied to reciprocating machinery fault detection. However, to the best knowledge of the author, JTFA has not been applied to Diesel engine fault detection.

1

B. RESEARCH OBJECTIVES

The primary objective of this research was to develop and test methods to detect faults in a Diesel engine while it is operating. This will provide the tools necessary to implement CBM for Diesel engines.

A secondary objective was to develop a research facility capable of supporting a wide range of future engine studies.

C. RESEARCH METHOD

The engine is a complex system of interconnected parts. A fault in one part directly impacts the movements of others as the effects are transmitted throughout the machine. This interconnectivity makes engineering modeling very difficult. If the system was modeled there would have to be assumptions and simplifications which may introduce errors of sufficient magnitude in the output of the model, resulting in low confidence in the prediction without experimental confirmation.

By setting up an actual engine and introducing faults in a laboratory facility these modeling errors can be avoided. Another advantage of using a laboratory setting is the ability to repeat tests several times to validate the consistency of the results. Working in a engine testing facility, there is easy access to the engine for introducing faults and collecting data. The engine testing cell also provides a safe testing environment, if a fault causes catastrophic failure of the engine.

To accomplish the fault detection, advanced measurement technology and advanced signal analysis techniques were applied. The engine internal cylinder pressure and engine vibration data were collected. JTFA was used to evaluate the vibration data.

Of course there are many different types of engine faults. They can occur individually or in any number of combinations. For this research it was desirable to introduce a simple measurable fault without causing serious damage to the engine. There were two faults that were considered; injection timing and exhaust valve clearance. They are both adjustments normally checked during an engine tune up. The injection timing fault was selected since the timing tool has a micrometer for accurate measurement of the timing dimension for repeating the tests.

D. ORGANIZATION

Chapter II contains background information and a literature review. A discussion of maintenance methods, vibration analysis techniques and applications are provided. Background for JTFA including historic development and discussion of two popular methods is presented. Current research involving reciprocating machinery vibration analysis is reviewed.

Chapter III contains a discussion of the experimental setup and the engine fault which was introduced. The engine, dynamometer test stand, instrumentation and data collection equipment are described.

Chapter IV provides discussion of the results. Both cylinder pressure and engine vibration results are presented. The JTFA results are presented and the six different algorithms are evaluated.

Chapter V contains the conclusions and recommendations. The success of the engine fault detection is discussed. Recommendations for further study and process improvements are presented.

II. BACKGROUND

A. PERIODIC MAINTENANCE

U.S. Navy Fleet Maintenance in the past has been based on regularly scheduled overhauls. The intent of this method is to avoid failures during operation by overhauling the equipment on a periodic basis. The timing of the overhaul interval is set on a conservative basis so that significant machinery damage can be avoided. There are some drawbacks to this method. The maintenance is performed on some machines which are working fine and are not worn out. There are cases where the machine performance is worse after it has been overhauled. The key disadvantage of regularly scheduled maintenance is the cost of performing these regular overhauls. The cost is compounded due to the loss of availability during the overhaul. With the reductions in Defense budgets, maintenance dollars must be spent more efficiently.

B. CONDITION BASED MAINTENANCE

Condition Based Maintenance (CBM) is the most promising alternative to regularly scheduled maintenance. By monitoring the machinery condition, partial or complete repairs can be scheduled when they become necessary. Currently, The U.S. Navy is implementing an elementary form of CBM called Diesel Engine Trend Analysis (DETA). Which uses steady state performance measurements. A new system is under development called Integrated Condition Assessment System (ICAS).

It is very important to detect and diagnose faults before the equipment is seriously damaged to minimize the extent of the repairs needed. There are many parameters which can be monitored: operating pressures and temperatures; motor current flow; vibrations;

lubricating oil analysis and equipment noises, to name a few. The key to success is to be able to match common failure modes of the equipment to a particular signature or change in the parameters. It is the nature of mechanical devices to wear out slowly over their operating life. Normal wear and tear must be distinguishable from a major fault occurrence. Significant research and development is required to establish the knowledge base necessary to implement CBM.

C. VIBRATION ANALYSIS

Measurement of the vibrations of a machine is one of the most important tools available for CBM. Faults deep inside the machine can cause vibrations which are transmitted through the equipment structure. With sensitive accelerometers and high speed data acquisition the signals can be recorded. Then advanced signal processing techniques can be used to analyze the content of the signal. There are two different broad categories of machinery- rotating and reciprocating. Analysis techniques differ depending on the type of equipment.

1. Rotating Machines

The continuous spinning of rotating machines, such as gas or steam turbines, produces a very repeatable periodic vibration signal with a high signal to noise ratio. A rotating machine which is in excellent condition may display very little vibration. This leads to a signal with sharp harmonic content and low noise levels. When a fault develops, such as misalignment, imbalance, or bearing distress, the vibration levels typically increase dramatically. The primary analysis tool for rotating machines is spectral analysis. Many faults cause an increase in the magnitude of a particular frequency or change in phase. These frequencies are usually multiples of the fundamental operating frequency of the machine. However, instabilities tend to occur at the natural frequency of a structure.

6

Imbalance causes dominant vibrations at the fundamental rotating frequency. Misalignment causes vibrations at the fundamental and two times the fundamental frequency. The analysis of rotating machinery has been researched in detail. The Systems and Equipment Maintenance Monitoring for Surface Ships (SEMMSS) program uses these techniques to analyze rotating machines, Marshall [Ref. 1].

2. Reciprocating Machines

The vibration signal from a reciprocating machine is quite different than those delineated above for rotating machines. Vibrations from the reciprocating motion are non-stationary high energy bursts. The transmission of these vibrations through the many moving parts of the machine produces a great deal of noise in the signal. Spectral analysis can be used to evaluate some of the rotating parts of a reciprocating machine. However, it is ineffective evaluating the repeated transient signals of the reciprocating components. The time location of the frequency content of the signal is required to link individual parts of the signal with the effected component. [Ref. 2]

D. JOINT TIME FREQUENCY ANALYSIS

Joint Time Frequency Analysis (JTFA) is used to describe the energy content of a signal with respect to a time versus frequency distribution. If a signal with shifting frequencies, with respect to time, is analyzed using spectral analysis the time at which the frequencies occur is lost. JTFA is able to show when the frequencies occurred and what frequencies were present. If the signal contained periods with no output, JTFA will show when they occurred as well. Therefore, JTFA is an ideal tool for analyzing signals with dynamic frequency content, including transient signals. One of the best examples of this type of signal is human speech. It contains changing frequencies and pauses with no signal output.

7

The development of JTFA began in the 1940s. It was mostly driven by interest in analyzing human speech. The spectrogram or Short Time Fourier Transform (STFT) was the main tool used in the study of speech. In 1948 Ville [Ref. 3] derived a joint time frequency distribution for signal analysis that Wigner [Ref. 4] proposed in 1932 to study quantum statistical mechanics. This joint time frequency distribution is known as the Wigner-Ville distribution (WVD). Many more distributions have been developed in attempts to improve on the WVD. Each distribution has different characteristic advantages and disadvantages. There is no single best distribution for all possible signals. Therefore, each type of signal must be matched with the distribution which provides the desired analysis properties.

A detailed review of many of the joint time frequency distributions can be found in the article by Cohen [Ref. 5]. One of the new distributions, not covered in this article is the Adaptive Spectrogram. The development of the Adaptive Spectrogram is discussed in an article by Qian [Ref. 6]. The numerical algorithms used in the LabView Joint Time Frequency Toolkit are presented in the Users Manual [Ref. 7].

The following is a detailed presentation of the STFT and WVD. The advantages and limitations of each method are discussed. These two methods provide a general appreciation of the mathematics involved in JTFA. The other four distributions presented later in the results have similar equations resulting from minor variations.

1. Short Time Fourier Transform (STFT)

The STFT is obtained by breaking up the time signal $S(t)$ into many small segments called windows. Each window is centered at a particular point in time. The window slides along so that each data point in time can be analyzed. The Fourier Transform is taken for each window using the following equation:

8

$$S_t(\omega) = \frac{1}{\sqrt{2\pi}} \int e^{-j\omega t'} S(\tau) h(\tau - t) d\tau \qquad (2.1)$$

Where $h(\tau\text{-}t)$ is a windowing function centered at t. The energy density spectrum or spectrogram is:

$$P_S(t,\omega) = \left| S_t(\omega) \right|^2 \qquad (2.2)$$

The spectrogram provides an accurate representation of the signals energy versus time distribution. Unlike many of the other distributions, the spectrogram does not have any cross term interference. However, the time and frequency resolution of the STFT is limited. To improve the time resolution the width of the window must be shortened. This has the undesired effect of decreasing the frequency resolution. Therefore, it is impossible to obtain fine resolution for both time and frequency simultaneously. There must be a tradeoff between the two features to obtain optimum performance.

2. Wigner-Ville Distribution (WVD)

The WVD is obtained by adding up pieces made from the product of the signal at a past time multiplied by the signal at a future time. The equation for the WVD is shown below.

$$WVD(t,\omega) = \frac{1}{2\pi} \int S^*(t - \frac{1}{2}\tau) e^{-j\omega\tau} S(t + \frac{1}{2}\tau) d\tau \qquad (2.3)$$

The WVD produces a distribution with fine time and frequency resolution. This ability to localize the time and frequency content is the major benefit of the WVD. However, the product of the past and future signals introduces cross term interference (CTI) into the distribution. CTI is energy displayed in time and frequency locations where the original

9

signal does not contain that energy. It introduces false information into the joint time frequency display. Significant experience is required to analyze the WVD of a signal and separate actual energy features from the CTI.

With the introduction of noise into any part of a signal the CTI is dramatically increased. The noise in any portion of the signal has the effect of distributing itself throughout the WVD display. The displays become so cluttered with background noise that it becomes very difficult to determine which time-frequency energy peaks are real.

There are many other distributions which have been developed. The aim of many of them is to obtain the fine resolution of the WVD without getting the cross term interference. The Adaptive Spectrogram (ASD) is one of the more successful examples, as will be shown later.

E. CURRENT RESEARCH

There is a wide range of reciprocating equipment currently being studied. The list includes air compressors, pumps, refrigeration compressors and Diesel engines. Several studies have used JTFA to analyze machinery signals.

Rohrbaugh [Ref. 8] used JTFA to detect two different faults in a cam operated pump. The analysis included vibration data and motor current data. One fault was an overtightened packing gland on a pump pushrod. The other fault was a damaged pump discharge valve. Both faults were detected and each produced separate distinguishable signatures.

Zakrajesck [Ref. 9] reported on 4 years of research into transmission gear fault detection and damage assessment. This work is directed at improving the safety of helicopter rotor transmissions. Vibration data were analyzed using several methods including JTFA. The WVD was used to detect gear tooth damage from initial pitting to

tooth fracture. The WVD was found to contain too much information. Post-processing, which includes filtering, was recommended to separate the useful information from the CTI. The JTFA showed potential to evaluate the extent of the damage. The time frequency plots progressively changed as the amount of damage increased. The report concluded that no single analysis method was capable of detecting and assessing all of the gear fault types tested. It recommended that several of the methods, including JTFA, receive further study.

Diesel engine condition monitoring has been receiving increasing attention from engine manufacturers and diagnostic system vendors. O'Conner [Ref. 10] reports on the technology, methods and research being carried out by several engine manufacturers.

General Electric's Transportation Systems division manufactures diesel engines for locomotives. They are developing an expert diagnostic system incorporating the Diesel Engine Unit Condition Evaluator (DEUCE) developed by R.H. Lyon Corp. (Cambridge, Mass.). The DEUCE system is used to capture and analyze vibration signals. The vibrations are recorded from externally mounted transducers. The signals undergo sophisticated signal processing to obtain signatures of individual components within the engine. The signals are analyzed in the time domain not the time-frequency domain. The system has been proven in the lab to diagnose valve-seat impacts, fuel injection problems and broken or worn piston rings.

III. EXPERIMENTAL SETUP

A. EQUIPMENT

1. The Diesel Engine

The engine setup for this laboratory is a Detroit Diesel 3 cylinder 53 series shown in Figure 3.1. The engine characteristics are listed in Table 3.1. This particular engine, serial # 3D-68137 was manufactured in March 1970. It was used in a US Army 1-1/4 Ton Cargo Truck commonly called a "Gamma Goat". These trucks were phased out and 2 surplus engines were acquired in 1985. The paperwork with the engines indicated that they had been overhauled and were ready for use. During construction of the test cell several small problems were discovered and repaired. The problems ranged from a
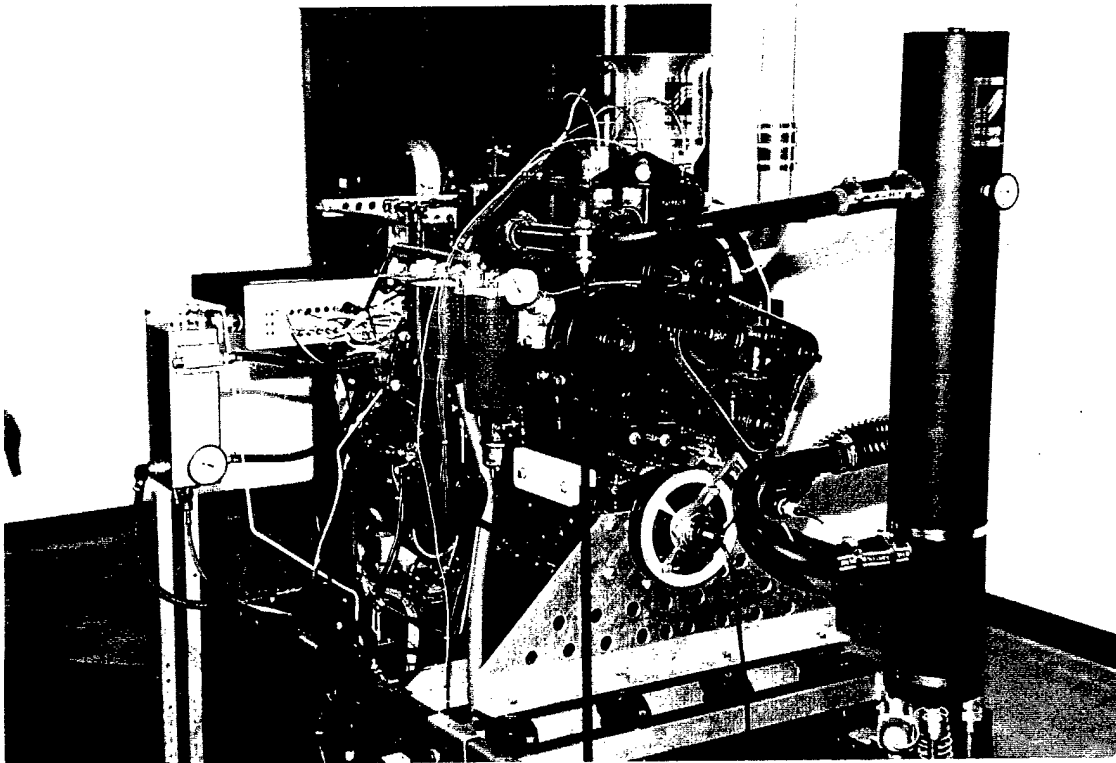
Figure 3.1 Detroit Diesel 3-53 Test Engine

13

Table 3.1 Engine Characteristics

Model	5033-5001
Number of Cylinders	3
Bore and Stroke	3.875 x 4.5 inches
Cylinder Displacement	53 cubic inches
Engine Displacement	159 cubic inches
Compression Ratio	21.0 : 1
Engine Type	Inline - 2 Cycle
Maximum Power Output	92 bhp
Maximum Power Speed	2,800 rpm
Peak Torque	198 foot pounds
Peak Torque Speed	1,500 rpm
Brake Mean Effective Pressure	83. psi

missing thermostat to the wrong type of fuel pump installed on the engine. Appendix A contains a list of all the mechanical problems encountered and the corrective actions taken.

This is a two stroke engine with a positive displacement air intake blower and 4 exhaust valves per cylinder. There is a gear train in the back of the engine which drives the blower, governor, fuel pump, camshaft and the balance shaft. On the front of the engine there are two counter rotating weighted disks mounted to the camshaft and the balance shaft. These disks are used to reduce the vibration of the engine during operation. The water pump mounted on the front right is driven by belts from the balance shaft. The air intake is fitted with a calibrated turbine meter to measure the air flow rate and temperature. The exhaust manifold has thermocouples positioned at each cylinder exhaust port. The exhaust passes from the manifold to a muffler. Then it goes to an 8 inch

14

diameter exhaust pipe running from the test cell to the roof of the building. Detailed performance curves and engine data provided by the manufacturer are given in Appendix B.

2. The Dynamometer

The engine is mounted on a Superflow 901 Dynamometer test stand. Figure 3.2 shows the dynamometer stand and the water brake. The dynamometer uses a water brake power absorber with maximum capacity limits of 1,000 hp and 10,000 rpm. The absorber capacity valve is set to 1 3/4 turns open for this specific engine. A torque measurement link is used to determine the power absorbed by the water brake. For this application the link was calibrated using static weights for the range of 0-212.4 ft lbs. The test stand measures fuel flow with a turbine meter. A mixing tower is mounted on the front of the stand to provide engine jacket water cooling.
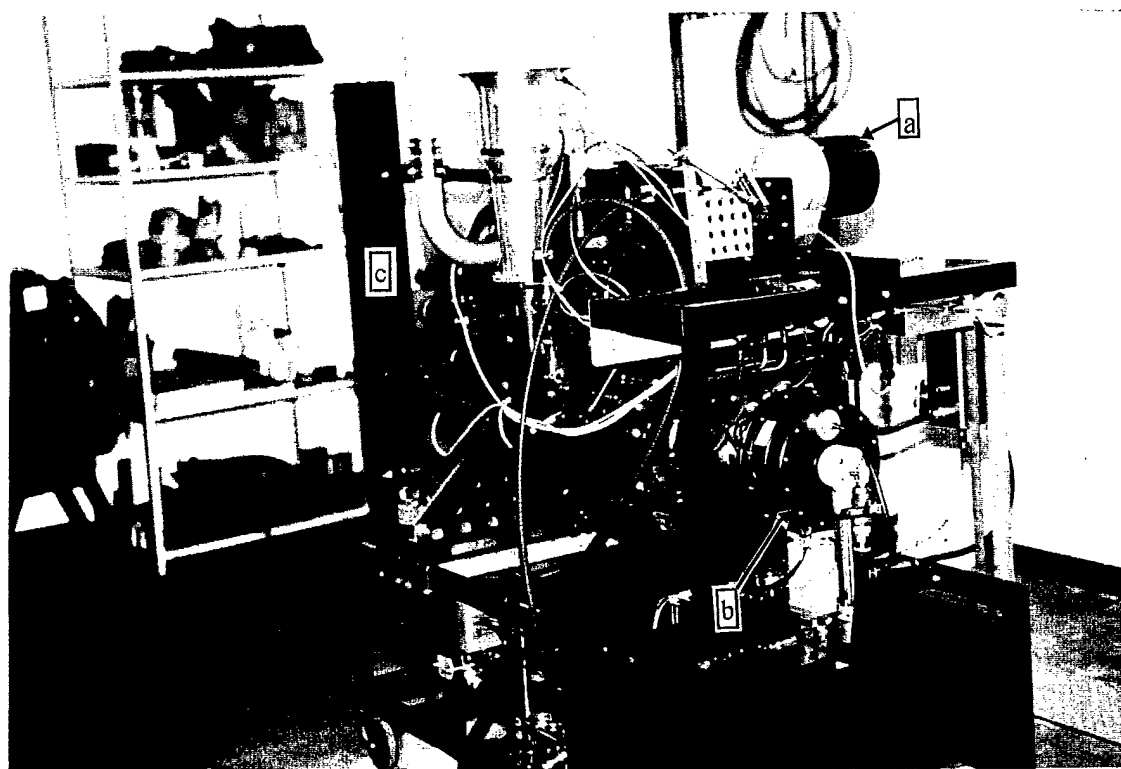
Figure 3.2 Superflow 901 Dynamometer Test Stand (a) throttle control servo (b) water brake assembly (c) jacket water cooling/mixing tower

15

The dynamometer control console, shown in Figure 3.3, is capable of both manual and automatic control of the engine speed and torque. The normal operating mode for a Diesel engine is throttle controlling speed and load controlling torque. In this mode the control console will automatically control the governor and the load control valve.

Appendix C contains detailed operating instructions for the engine, dynamometer and data acquisition system.
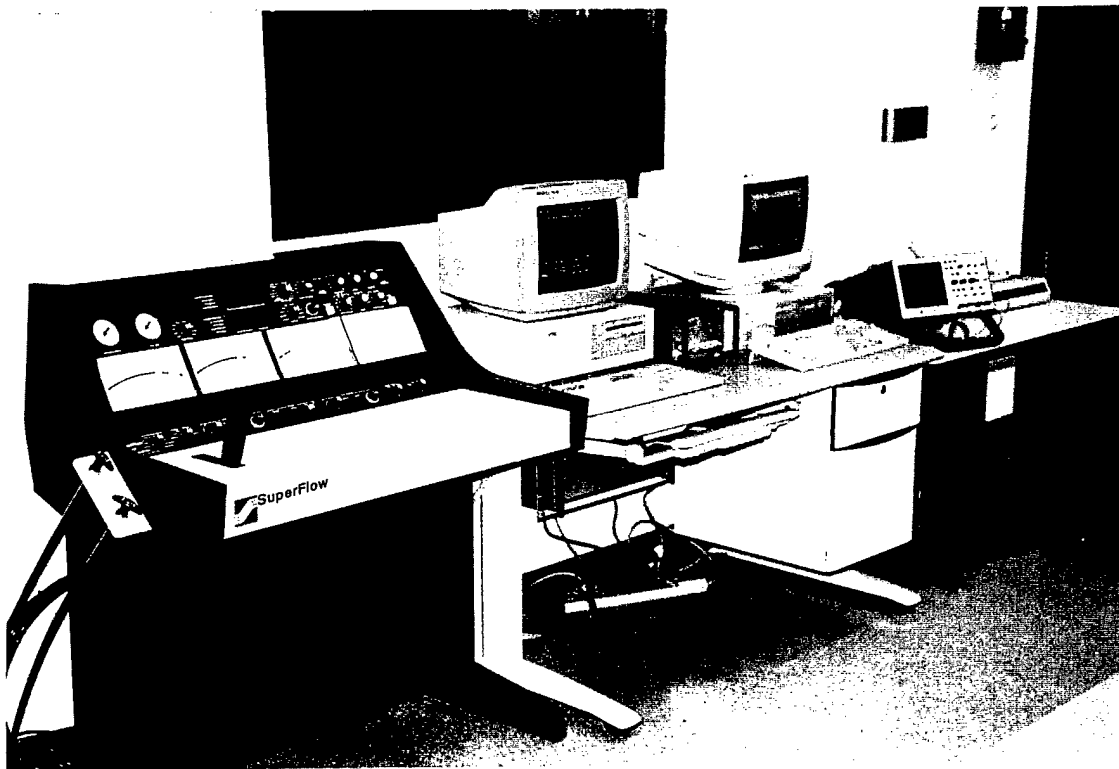
Figure 3.3 Dynamometer Control Console

3. Instrumentation

a. Cylinder Pressure Transducers

The pressure sensor is specially designed to perform in the high temperature environment of the combustion chamber. It has high frequency response to changing pressure necessary to capture the pressure rise and fall during a single

revolution. To gain access to the combustion chamber and mount the cylinder pressure transducers, a new cylinder head, from the V-6 version of the engine was installed. The new head had glow plug ports already in the casting. The transducers were ordered with the same thread size as the glow plug port threads. This provided easy installation and access to the transducers for maintenance. An added benefit of this method was a pressure tight seal around the transducer base. A glow plug is longer than the pressure transducer and projects into the combustion chamber about 0.75 inches. The pressure transducer is recessed 1.125 inches from the top of the combustion chamber. The port between the transducer and the combustion chamber is 0.2 inches in diameter. Figure 3.4 shows the new cylinder head and the location of the glow plug port.
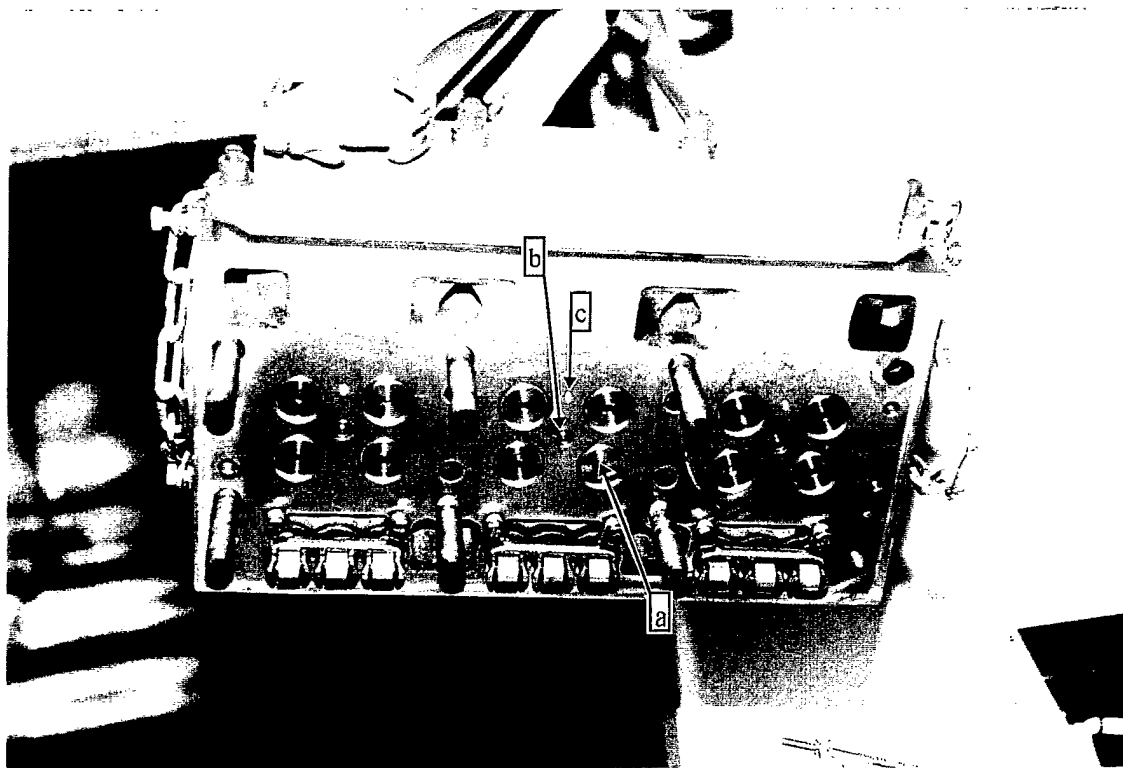
Figure 3.4 Cylinder head showing orientation of (a) exhaust valves, (b) fuel injector and (c) glow plug port

17

b. Vibration Transducers

The placement of the vibration transducers was expected to be very important. The vibration signals measured are critically dependent on the transmission path from the source to the transducer. The natural frequency and damping characteristics of the structure that the transducer is attached to directly affects the measured signal. The source in this case was the combustion process inside the cylinder. The cylinder pressure, P(t), increases rapidly as the fuel is injected and burned. The cylinder walls and the cylinder head are subjected to dynamic loading from P(t). The resulting vibrations travel outward through the block and head assemblies. There were many transducer mounting locations considered on the valve cover, block and head. The valve cover is a thin stamped steel structure attached to the head by four small screws. Since it is further away from the source, it was quickly ruled out. Magnetic mounts for the cylinder head and block were rejected since positioning would not be easily repeatable and may fall off or shift during operation. Additionally, the block is manufactured from aluminum not iron so magnetic mounts will not work.

To achieve as direct a path as possible, the transducers were mounted on the cylinder head bolts. Figure 3.5 shows the cylinder head with the valve cover removed. Figure 3.6 and 3.7 show close up views of the cylinder head bolts with the transducers mounted on them. Figure 3.8 shows a transducer mounted on top of a valve rocker arm bridge bolt head. The head bolts provide the strength to maintain the seal between the cylinder block and the head. Therefore, they are very close to the source of the vibrations. The bolt heads were center tapped and threaded to install a triaxial transducer mounting cube. One bolt was set up with three transducers in a triaxial mounting arrangement. Two other bolts, around the first cylinder, each had a single transducer mounted in the vertical direction. The last transducer was mounted on the top of a rocker arm bracket bolt in the vertical direction. Since the engine is an in line type, the reciprocating action of

18

the engine causes the largest vibrations in the vertical direction. Therefore, the majority of the transducers were mounted in the vertical position. Once the transducers were mounted, they were sealed in RTV silicone sealer to prevent engine oil from entering the electrical connections.
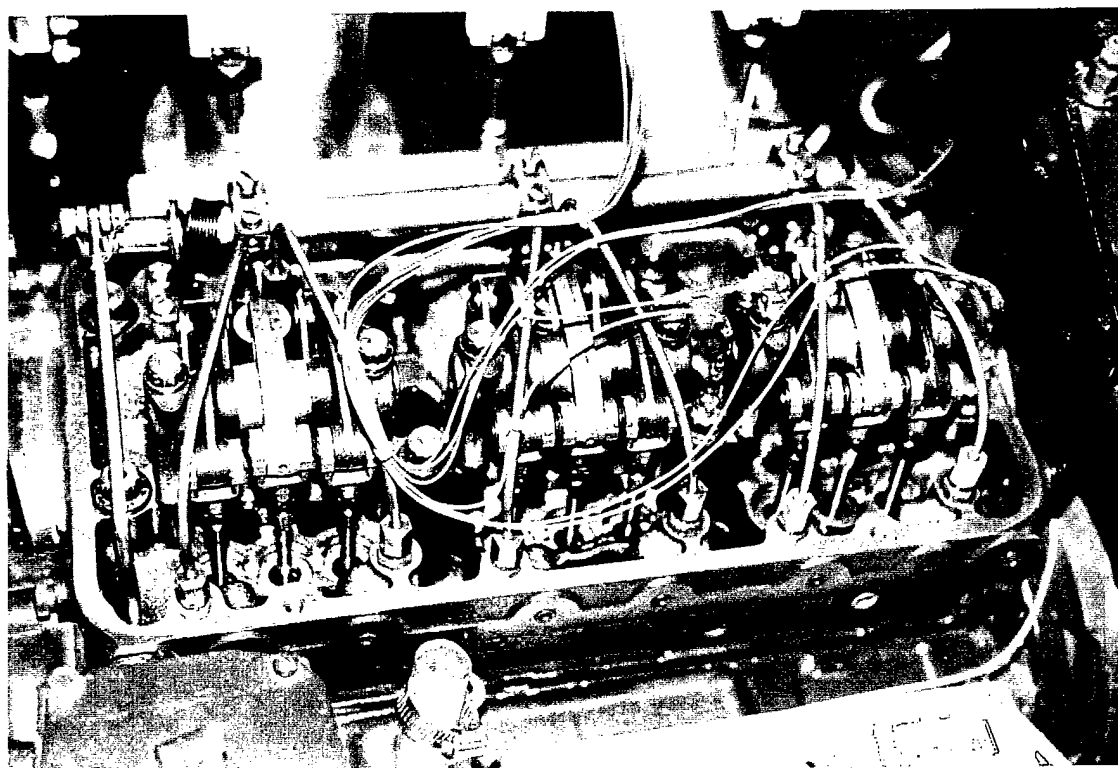
Figure 3.5 Cylinder head with the valve cover removed showing vibration transducer mounting locations and wiring
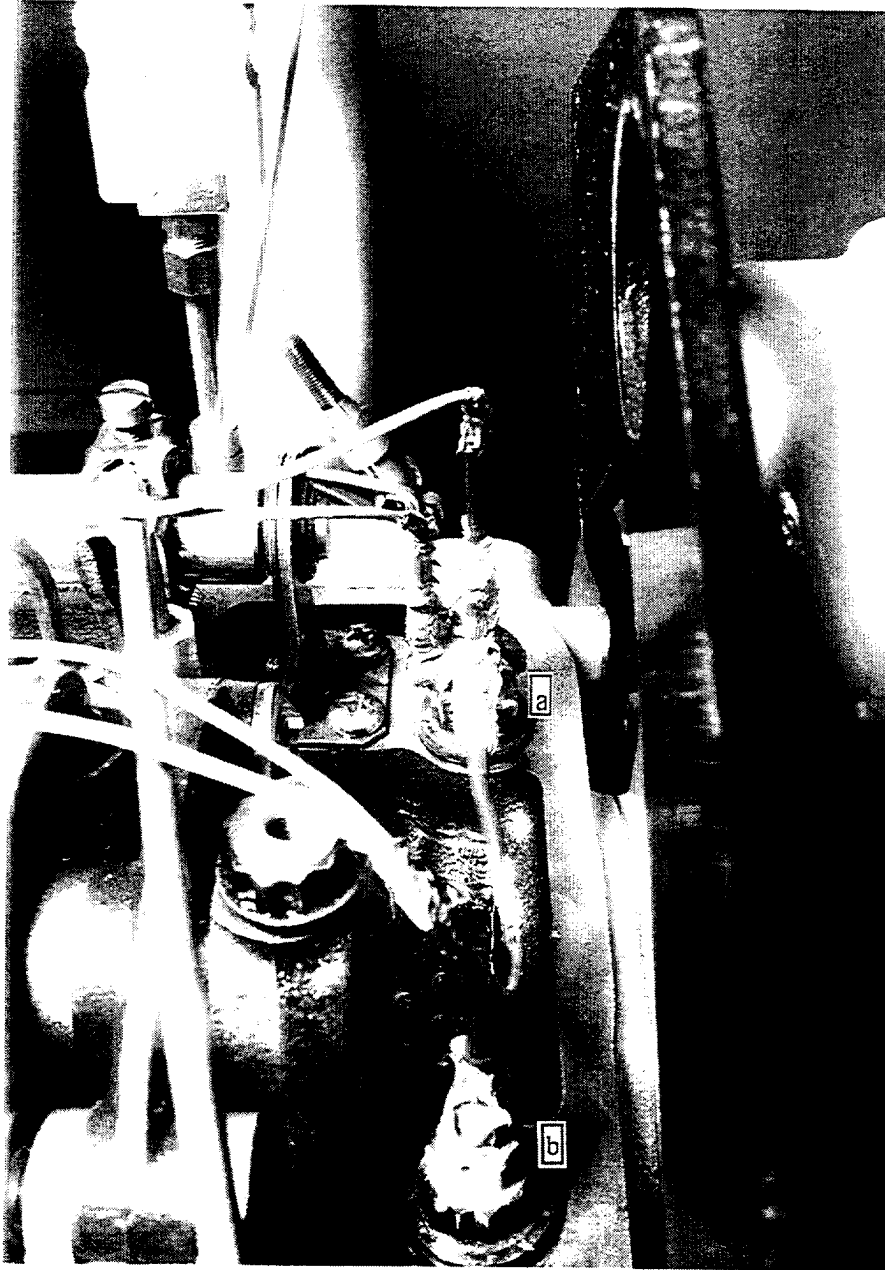
Figure 3.6 Vibration transducers shown sealed in RTV (a) Triaxial transducer mounting
(b) single vertically mounted transducer
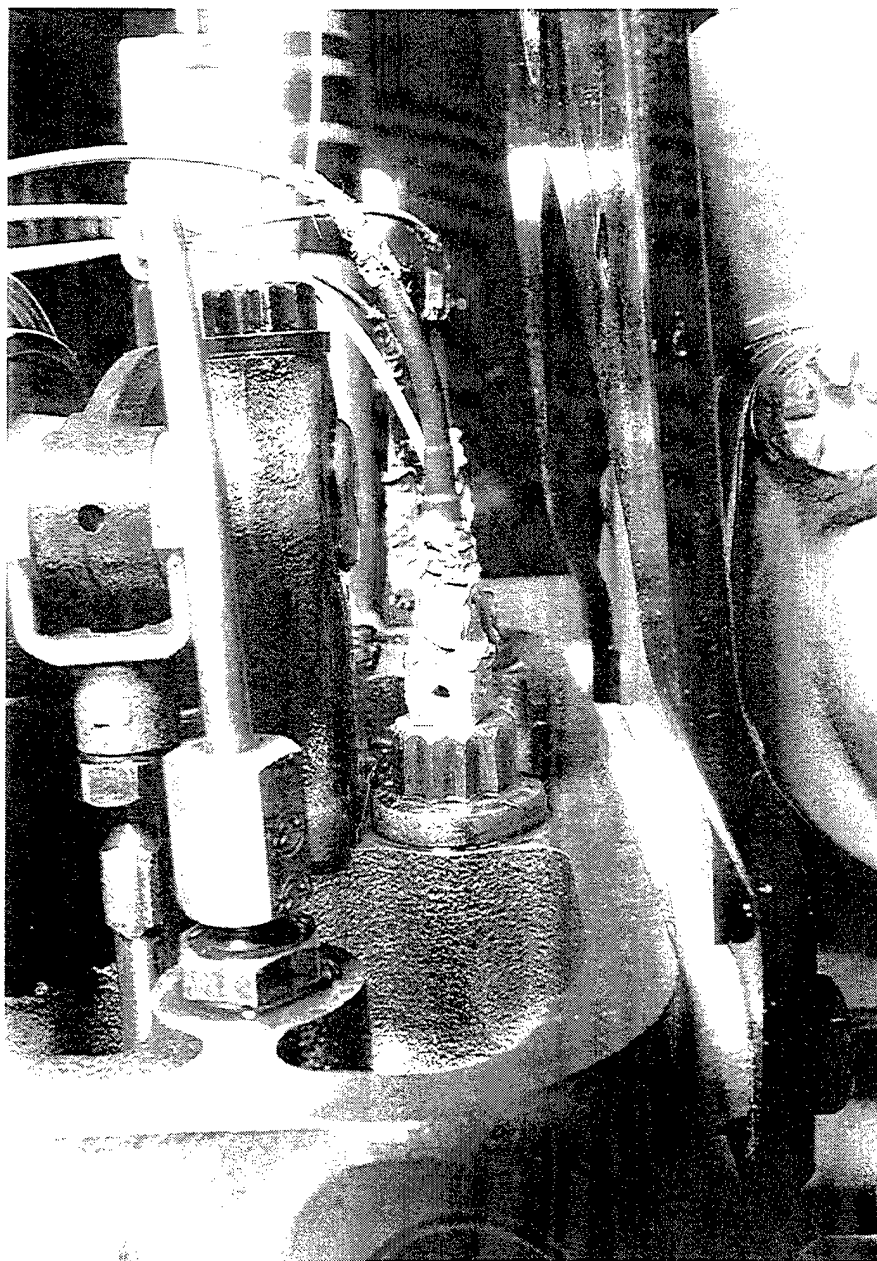
Figure 3.7 Close-up view of the vertically mounted vibration transducer
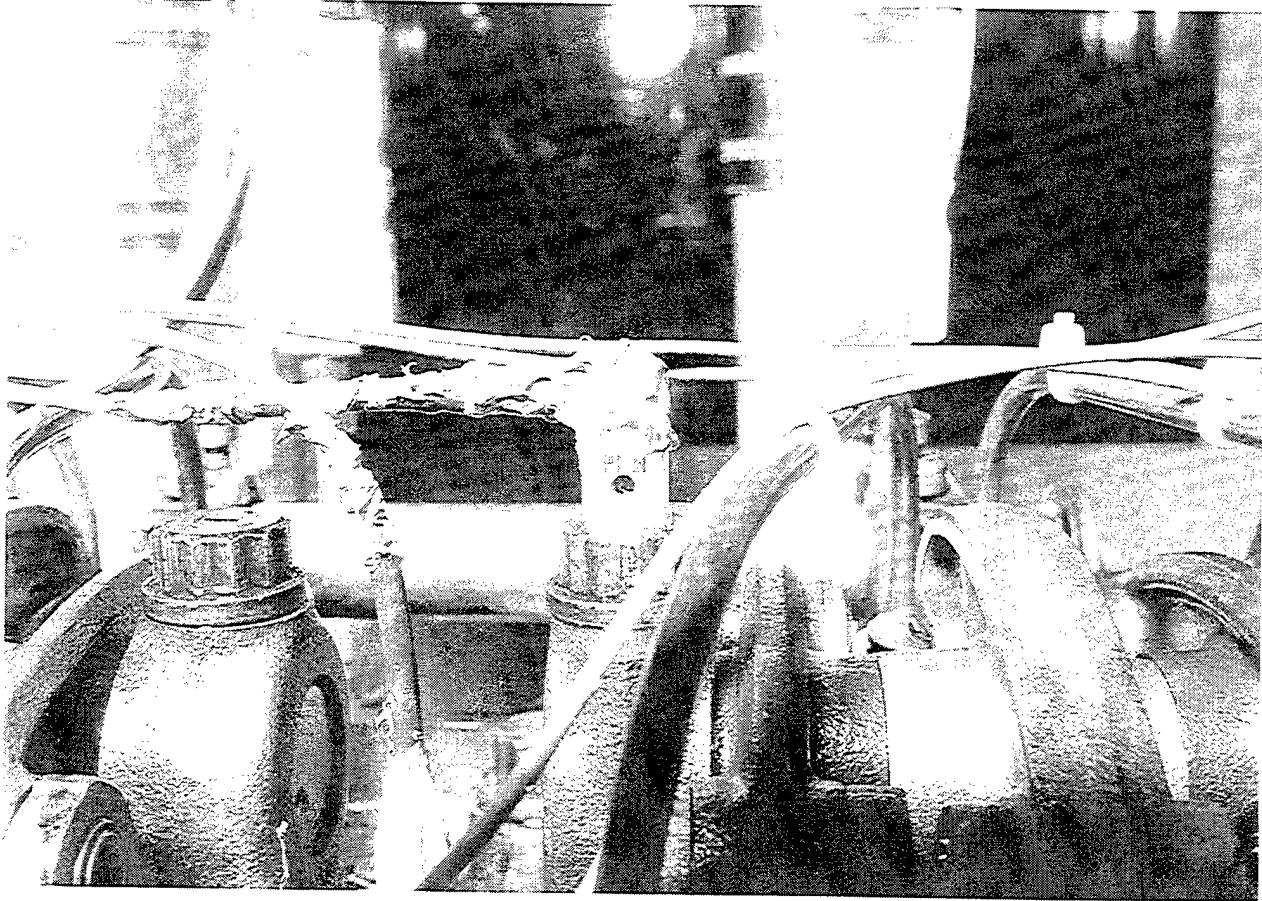
Figure 3.8 Vibration transducer mounted on a rocker arm bridge bolt

4. Data Acquisition

The engine cycle analyzer (ECA) performs the function of data acquisition and display. The ECA is designed for analyzing the Cylinder Pressure vs. Volume curve for an internal combustion engine. However, the data acquisition capabilities are flexible so data other than cylinder pressure can be recorded. There are three major components; an optical encoder, signal filter for the vibration signals and a computer based data acquisition system.

The optical encoder shown in Figure 3.9 is mounted in front of the crankshaft pulley. It provides a pulse, once each revolution, to indicate the location of top dead

center on the first cylinder. It also provides separate pulses every tenth of a degree or 3,600 pulses per revolution to trigger the data acquisition. Thus the crankshaft angular position is known throughout the revolution. This information is used with the dimensions of the connecting rod, cylinder bore and stroke to calculate the volume of the cylinder at each data point.
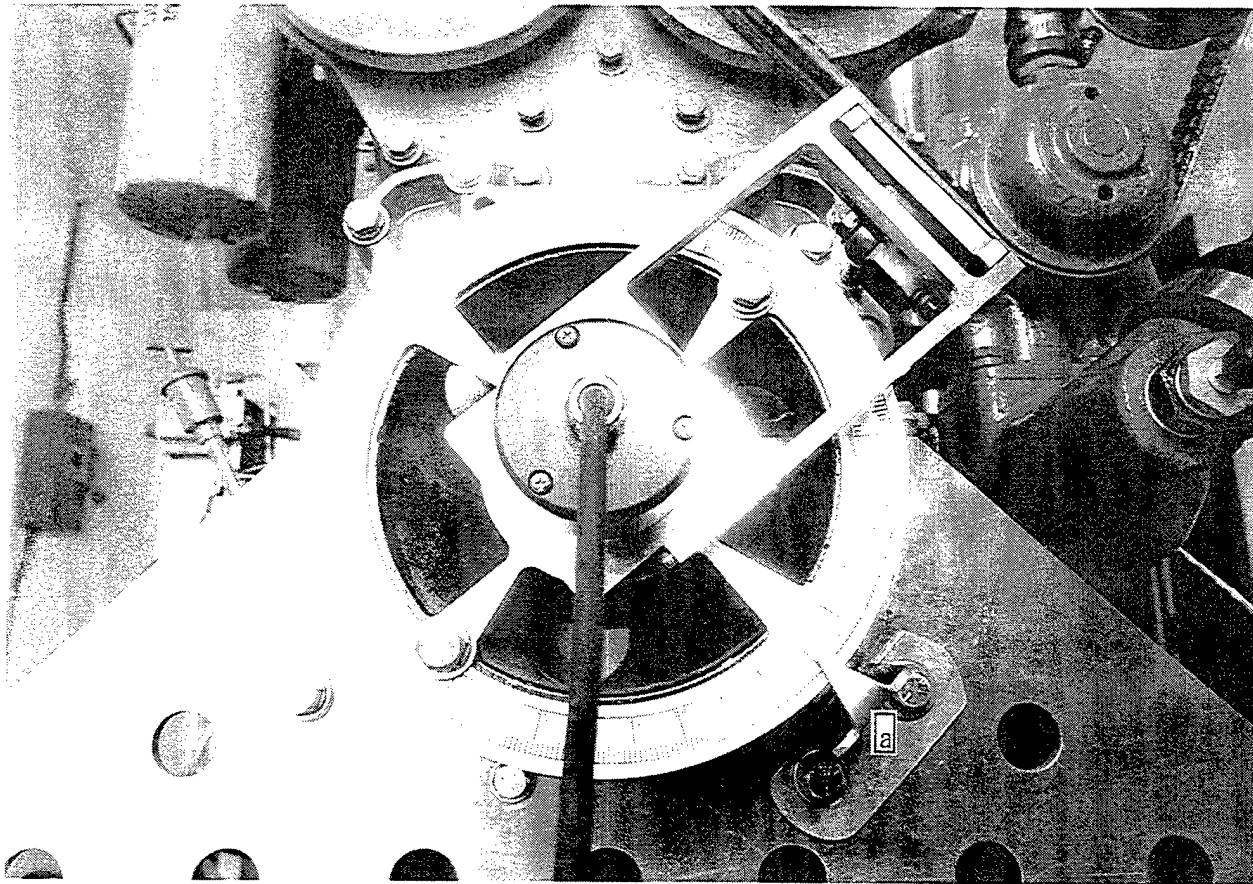
Figure 3.9 The optical encoder mounted concentric to the crankshaft pulley (a) pointer and timing ring used to align the optical encoder

For the vibration data, all of the signals were filtered before converting from analog to digital. The data sampling rate was 108 khz, which corresponds to an engine speed of 1,800 rpm. A low pass filter was used with a 30 khz setting to prevent aliasing. This permits the frequency content of the signals to about 15 khz to be analyzed.

The computer based data acquisition system included an Analog to Digital (A/D) sampling card and a 486 DX2 66 Mhz desktop computer. The A/D sampling card was a 12 bit card capable of recording 4 channels at 125 khz sampling rate. Any $\pm$ 5 volt sensor signal can be fed to the system. For this research one pressure sensor and one vibration sensor were used for data collection.

The ECA computer software for data acquisition allowed the user to capture data from a number of revolutions. Then they could be averaged together to obtain a single representative cycle. By limiting the number of channels in use, the total number of revolutions of data collected increased to 69. These 69 revolutions or cycles were then averaged and stored in data files. These time domain data files could be displayed using the ECA software. For the Joint Time Frequency Analysis, the vibration data files were loaded into the LabView JTFA Toolkit software. Appendix D contains instructions for data collection and an example of a data file.

B. FUEL INJECTION TIMING FAULT

There are many different types of engine faults possible. For this study the possibilities were limited to prevent severe damage to the engine or the test stand. Faults affecting the combustion process were desired. Two possible combustion faults were considered, a timing fault and an exhaust valve leak. Both of these faults can be imposed by adjusting the rocker arm linkages. The timing fault was selected because it is easily measured and repeatable. Errors in injection timing are a common cause of inefficiency.

1. Description of the Fuel Injection Process

The fuel injection for the Detroit Diesel 3-53 is accomplished using a direct mechanical injector. The injector is actuated by a rocker arm acting on the injector plunger. As the plunger moves it meters the fuel and provides the pressure necessary to spray an atomized mist into the combustion chamber. The amount of fuel injected is controlled by a fuel rack which is connected by a linkage to the governor. The fuel rack position can be varied from no fuel to maximum. A manual pull cable on the control console forces the fuel rack to the no fuel position during a normal stop.

During a normal combustion cycle fuel injection begins before the piston reaches Top Dead Center (TDC). This is to allow time for the fuel to mix and burn. As the piston reaches TDC the crankshaft rotation corresponds to very small changes in the piston's position. Therefore, the volume in the combustion chamber is almost constant during the short rotational period near TDC. The burning fuel causes a rapid increase in the combustion chamber pressure. The pressure peaks just after TDC and falls off as the piston moves down increasing the combustion chamber volume.

To provide better understanding of the order and overlap of the events from all of the engine cylinders, a map of engine events with respect to crankshaft angle is provided in Figure 3.10. The events displayed are intake port, exhaust valve and fuel injector movements. This map was developed by turning the engine over by hand and recording the angular position of each event. All of the angular positions are referenced to 0° corresponding to TDC on number 1 cylinder. The firing order of the engine (2-1-3) can clearly be seen. Number 2 cylinder events occur 120° before number 1 cylinder and number 3 cylinder events occur 120° after number 1 cylinder.

25
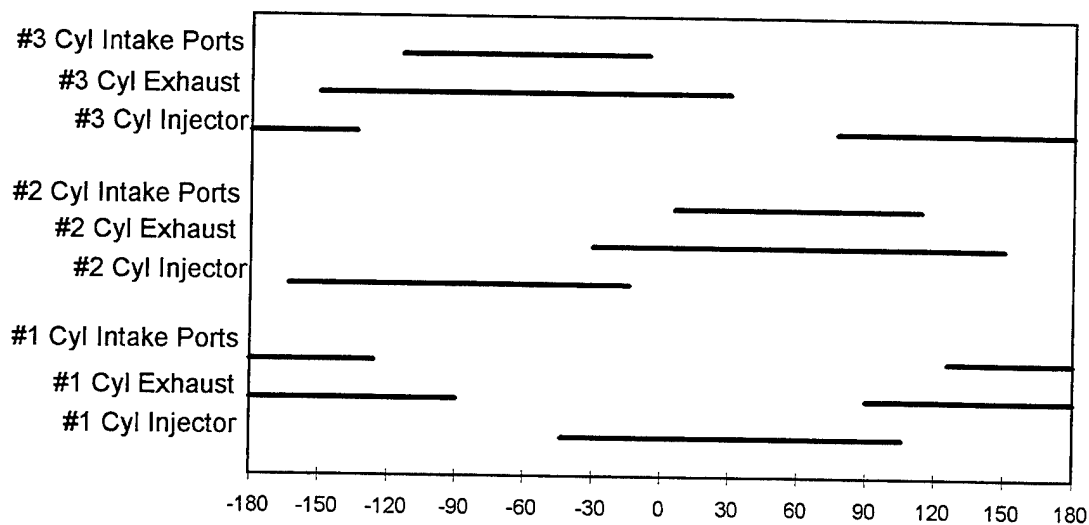
Figure 3.10 Engine Event Timing Map

Now take a closer look at each event for number 1 cylinder. Starting at -180°, the piston is at the bottom of its stroke and the intake ports and exhaust valves are fully open. As the piston moves up, it gradually covers up the intake ports in the cylinder wall. At -126° the crown of the piston closes off the intake ports. A few degrees later the piston rings will fully seal off the intake ports. Next the exhaust valves, which are controlled by the camshaft, close at -90°. At -43° the fuel injector plunger begins its downward stroke. A portion of the initial injector movement is used to pump and measure the correct amount of fuel to be injected. The point of actual fuel injection into the cylinder could not be observed. The piston passes through TDC and begins to move down. The fuel injector plunger reaches its maximum downward stroke at 31°. The plunger moves back up refilling with fuel and preparing for the next cycle. The exhaust valves crack open at 90°. Finally the piston motion uncovers the intake ports at 126° and the cylinder purging begins.

26

2. Expected Effects of a Timing Shift

Injection timing is a critical factor in the efficient running of a Diesel engine. When the timing is set correctly the peak pressure occurs 3-6 crankshaft degrees after TDC. This is when the pressure is acting on the piston and can produce useful work. If the timing is advanced the peak pressure can shift to before TDC and will be providing resistance to the normal piston movement. This results in a loss of work and higher stresses in the crank shaft and connecting rod. The amount of work done by each cylinder will become unbalanced as the other cylinders work to overcome the resistance of the faulty cylinder and maintain the output power level.

When the timing is retarded the peak pressure will occur later after TDC and will reach a lower pressure peak than normal. The injection starts later and therefore the fuel has less time to burn before the piston starts to move down. This results in a lower work output from the effected cylinder. Again the other cylinders will assume a greater portion of the load, but the stress levels will not rise as much as the advanced timing case.

3. Actual Fault Introduction

During an engine tune up the initial height of the injector plunger is checked and adjusted. The timing dimension, for the N50 injectors installed on this engine, is 1.460 inches. All of the injectors were initially set to this value using the procedure in the maintenance manual [Ref. 10]. The engine was operated to collect the baseline data. Four separate sets of data were taken at 1,800 rpm and 180 foot pounds torque. This operating point is approximately 90% of full load.

The test loading conditions must be at least 80% of the rated load [Ref. 2]. This will ensure smooth operation with minimum gearclash and torsional vibration. Under heavy loading conditions engine faults are more likely to be detected. Each cylinder must

carry an equal share of the load. If there is a fault, the load will become unbalanced and vibrations will show detectable differences compared to baseline vibration measurements.

The engine was shut down and then the timing dimension was checked. Due to thermal growth the dimension was 1.464 inches. The rocker arm pushrod was adjusted to obtain 1.474 inches. The timing was retarded 0.010 inches. Then the engine was operated again. Another 4 sets of data were recorded at the same operating point. All of the data was collected and prepared for analysis.

IV. RESULTS

A. CYLINDER PRESSURE DATA

The data for the #1 cylinder pressure are plotted in Figure 4.1 and Figure 4.2. Figure 4.1 shows the complete engine cycle for one baseline data set and one timing fault data set. The bottom axis is the crankshaft angle from -180° to +180°. Several engine events are clearly distinguishable. Starting from the left, the intake ports and the exhaust valve are both open. The initial pressure level is due to the air intake blower forcing air through the cylinder. At -120° the intake ports are closed off by the movement of the piston and the pressure in the cylinder drops to atmospheric pressure. At -110° the exhaust valves close and the pressure begins to rise. The pressure peaks just after TDC. The baseline curve has a higher peak pressure than the timing fault curve, as expected. The pressure curves then fall as the piston moves down in the cylinder. At +110° the exhaust valves open and the pressure drops to atmospheric pressure. The intake ports open at +140° and air is again forced through the cylinder by the blower.

In Figure 4.2 two sets of baseline data and two sets of timing fault data are plotted. The bottom axis is adjusted to display the firing of the first cylinder. The four curves are nearly identical until the fuel injection occurs. The pressure rise associated with combustion is clearly visible. There is a 2° difference in the start of combustion between the baseline curves and the timing fault curves. The peak pressure point for the timing fault curves has shifted to the right and is 25. psi lower.

29
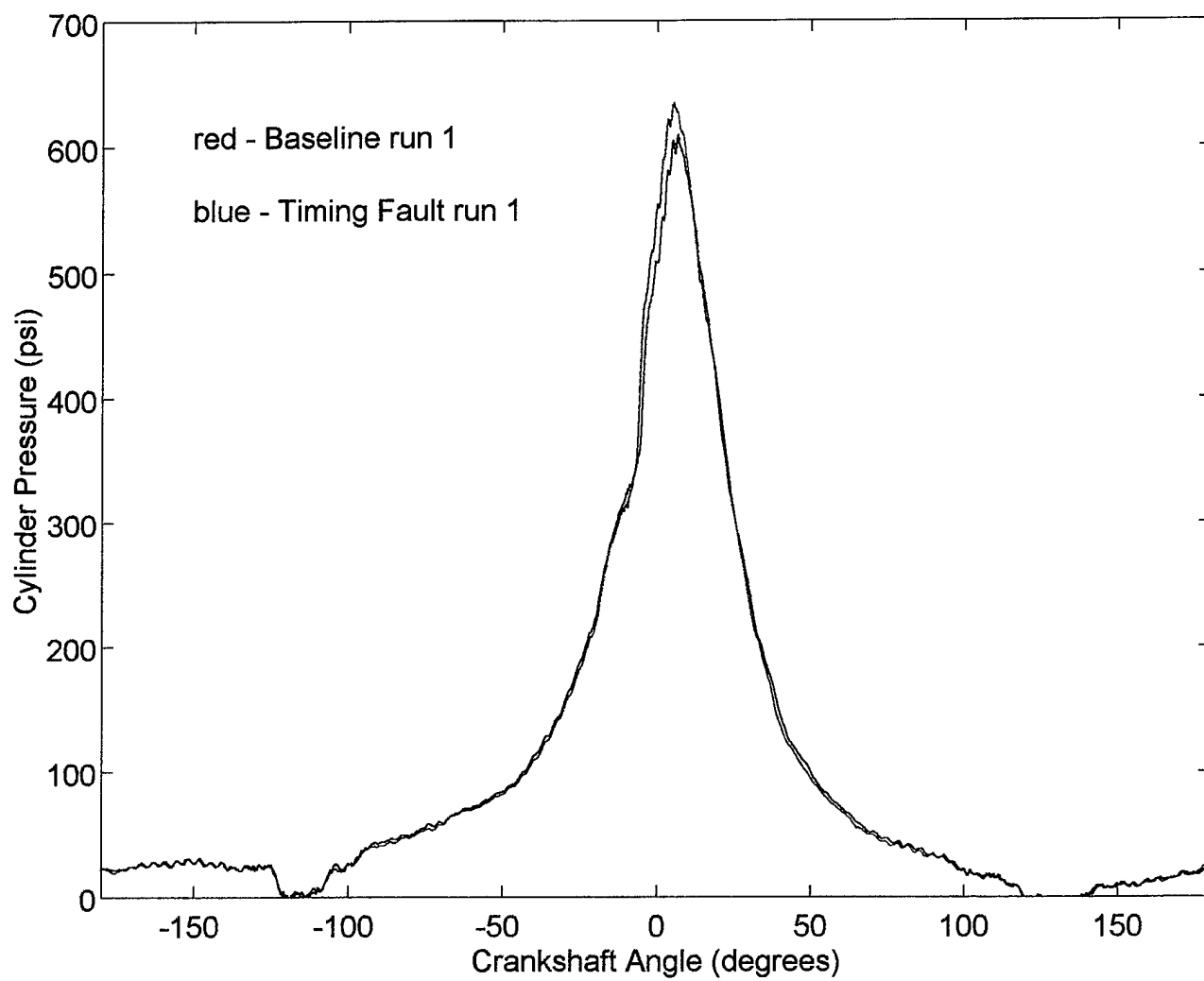
Figure 4.1 Cylinder pressure data plot for the complete revolution
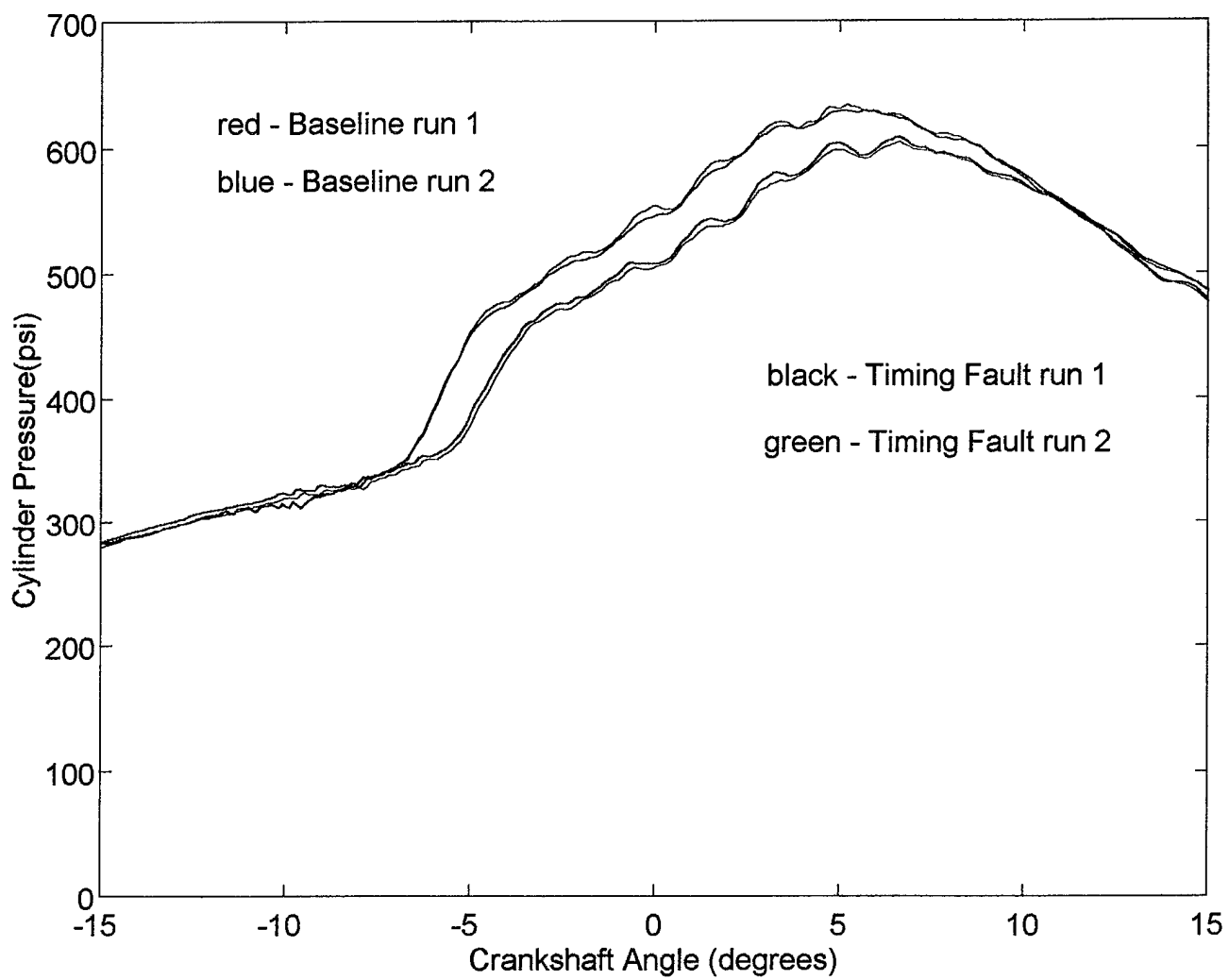
Figure 4.2 Cylinder pressure detailed plot

B. VIBRATION DATA JOINT TIME FREQUENCY ANALYSIS

The following figures and discussion are included to demonstrate each of the six types of JTFA distributions. All of the data were collected from one vibration transducer location, the vertical transducer on the triaxial mount shown in Figure 3.6 on page 20. The engine operating setpoint was 1,800 rpm and 180 ft lbs load. One data set for the baseline condition (upper figure) and one set for the timing fault condition (lower figure) were selected for analysis and display see Figure 4.3 and 4.4. Each of these figures share a common layout. The lower block with the green trace is the time domain signal of the vibration transducer. There are three bursts of vibrations resulting from the three cylinders firing in one complete crankshaft revolution. The firing order for the cylinders in this display is 2-1-3. Directly above the time domain signal is the Joint Time Frequency Distribution display. The frequency scale is shown to the right. The color bar to the left indicates the magnitude of the JTFD plot. The peak magnitude is 0 dB and is shown in white. The lowest magnitude is -50 dB relative to 0 dB and is shown in black.

1. Wigner-Ville Distribution (WVD)

Figure 4.3 shows the WVD of the baseline vibration signal. The timing fault condition vibration signal is shown in Figure 4.4. These WVD figures show very fine time and frequency resolution. However, the cross term interference and noise levels of the signals causes the display to be very cluttered. Except for the main energy peak at 1 khz and 0.0165 seconds, it is difficult to determine which frequencies are truly present in the signal. The WVD provides little or no useful information in determining the differences between the baseline and timing fault signals.

32

Figure 4.3 Wigner-Ville Distribution of the engine baseline vibration signal

Figure 4.4 Wigner-Ville Distribution of the engine timing fault condition vibration signal

33

2. Gabor Spectrogram

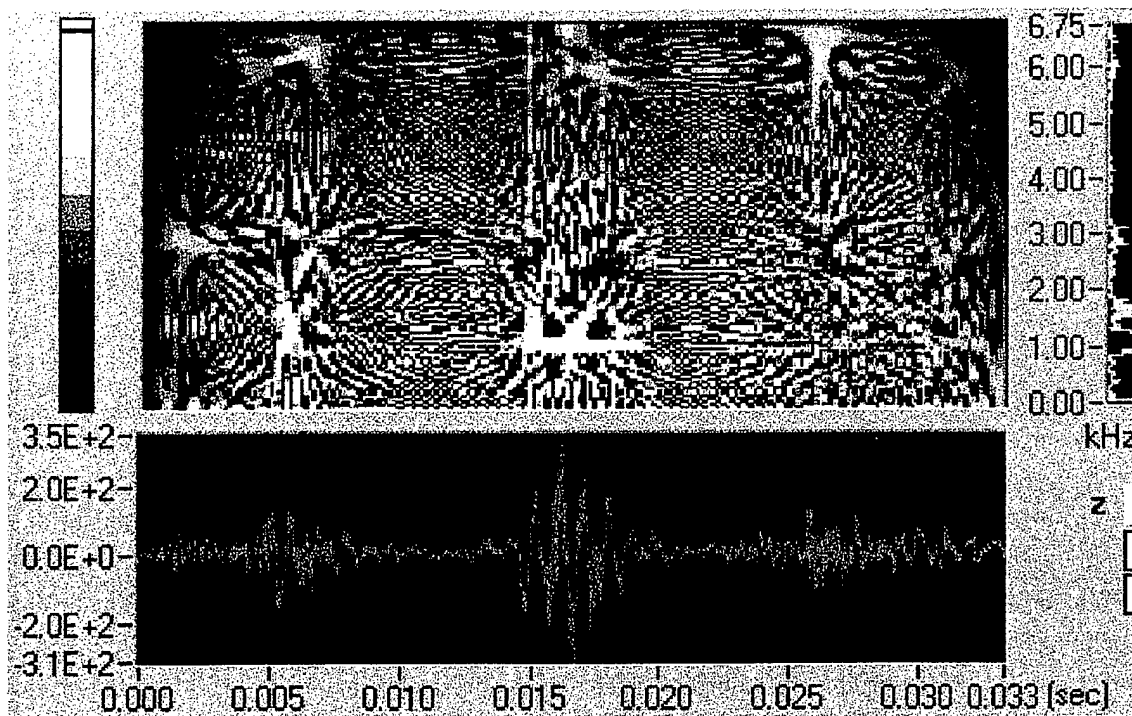Figure 4.5 shows the Gabor Spectrogram of the baseline vibration signal. The timing fault condition vibration signal is shown in Figure 4.6. The Gabor representations do not have the fine time and frequency resolution displayed in the WVD figures. The effects of cross term interference and noise are reduced but still present. Again there is little detectable difference between the baseline and timing fault signal spectrograms.

3. Short-Time Fourier Transform Distribution (STFT)

Figure 4.7 shows the STFT of the baseline vibration signal. The timing fault condition vibration signal is shown in Figure 4.8. The STFT does not have any cross term interference, but does show the background noise level in the dark orange-red areas. Concentrating on the center of the time domain where the first cylinder is firing at 0.016 seconds, there are some differences between the baseline and timing fault signal displays. The energy peak at 3 khz appears to have shifted to the right 0.003 seconds. The 6 khz energy peak magnitude has a lower value in the timing fault distribution than the value in the baseline distribution. The fundamental problem with the STFT is that tradeoffs must be made between time resolution and frequency resolution. However, this method does provide a useful display of the time and frequency content of the signal.

4. Cone-Shaped Distribution (CSD)

Figure 4.9 shows the CSD of the baseline vibration signal. The timing fault condition vibration signal is shown in Figure 4.10. These CSD figures show good frequency resolution but poor time resolution. The horizontal stripes provide narrow frequency band information but do not distinguish the location in time clearly. The effects of cross term interference and noise are present again, but less than the distortion levels in the WVD. The CSD provides little or no useful information in determining the differences between the baseline and timing fault signals.

34

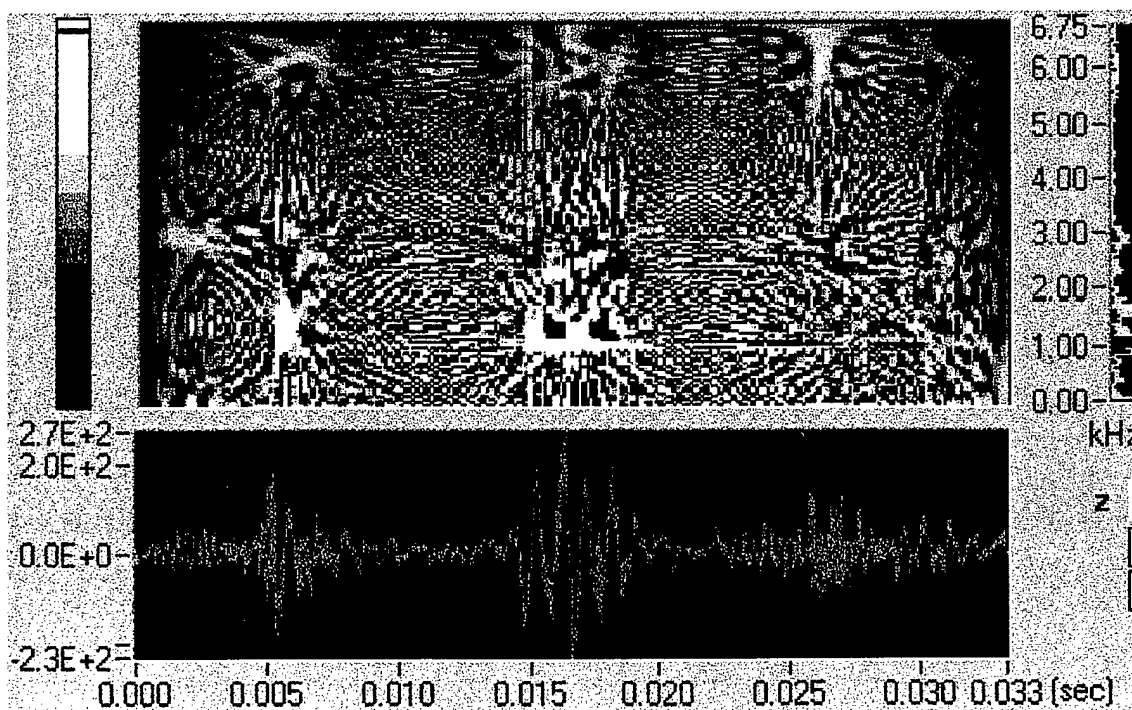Figure 4.5 Gabor Spectrogram of the engine baseline vibration signal
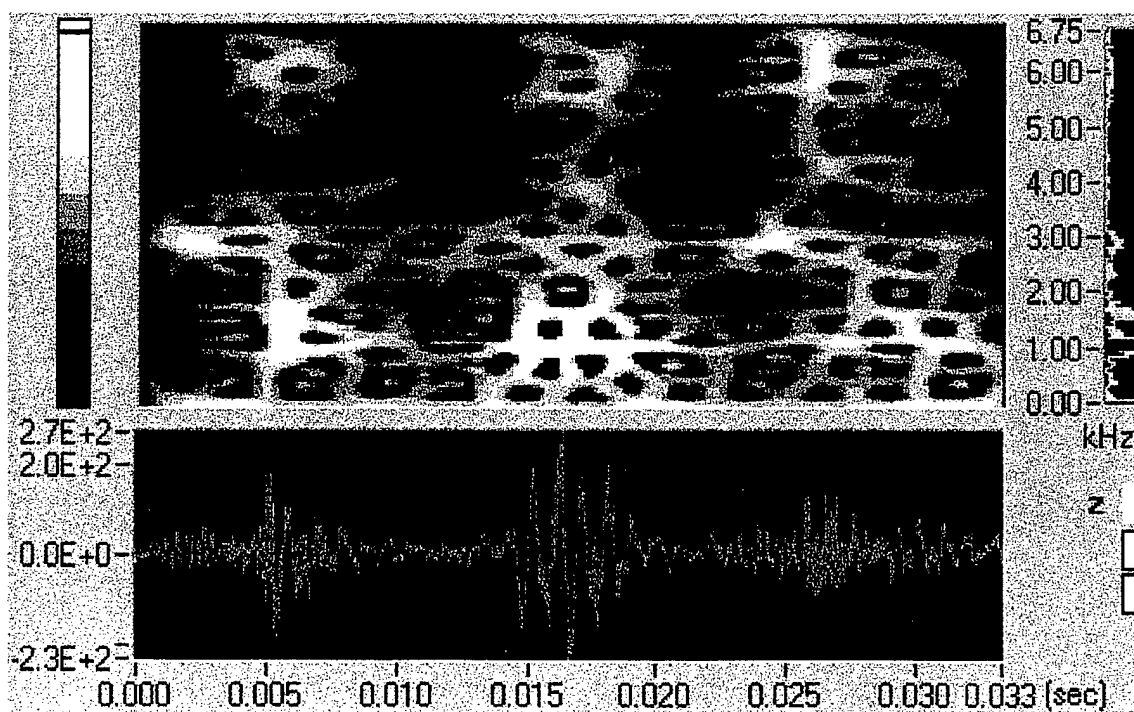
Figure 4.6 Gabor Spectrogram of the engine timing fault condition vibration signal

35
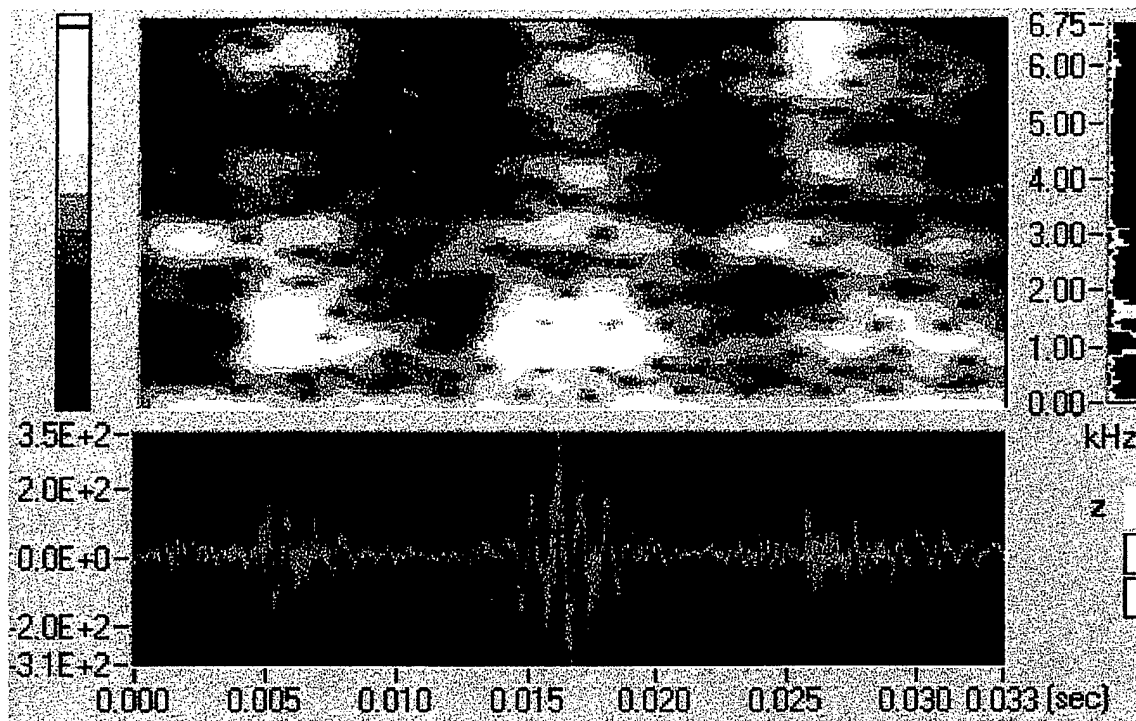
Figure 4.7 Short-Time Fourier Transform of the engine baseline vibration signal
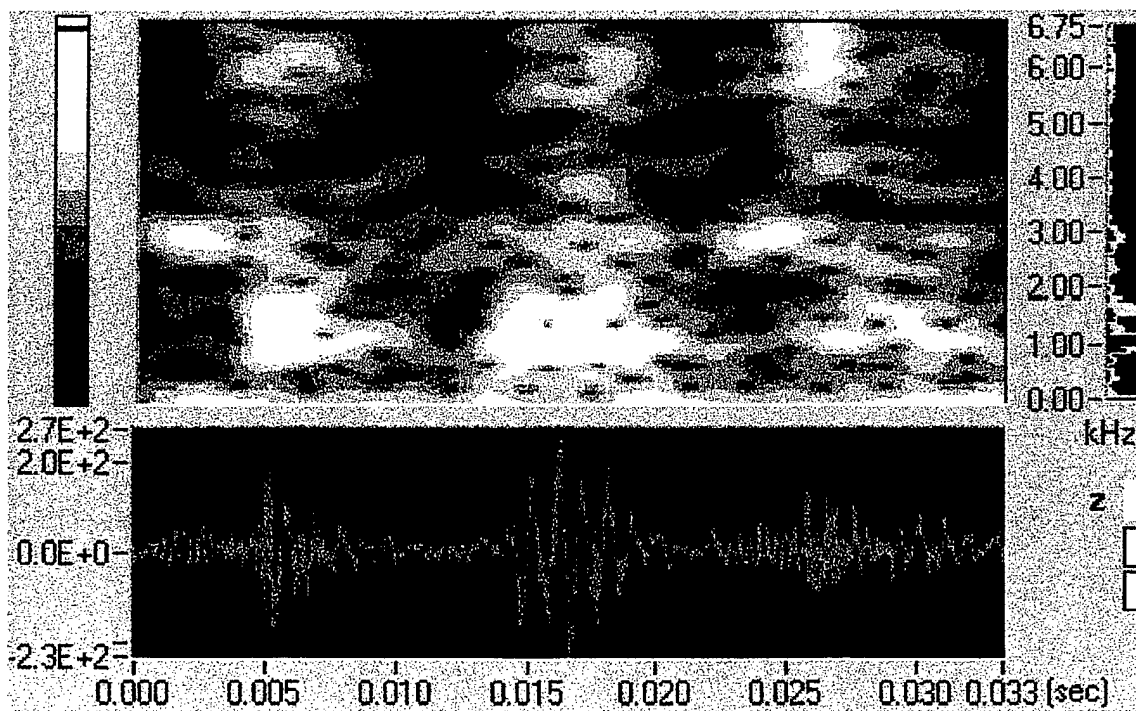
Figure 4.8 Short-Time Fourier Transform of the engine timing fault condition vibration signal

36
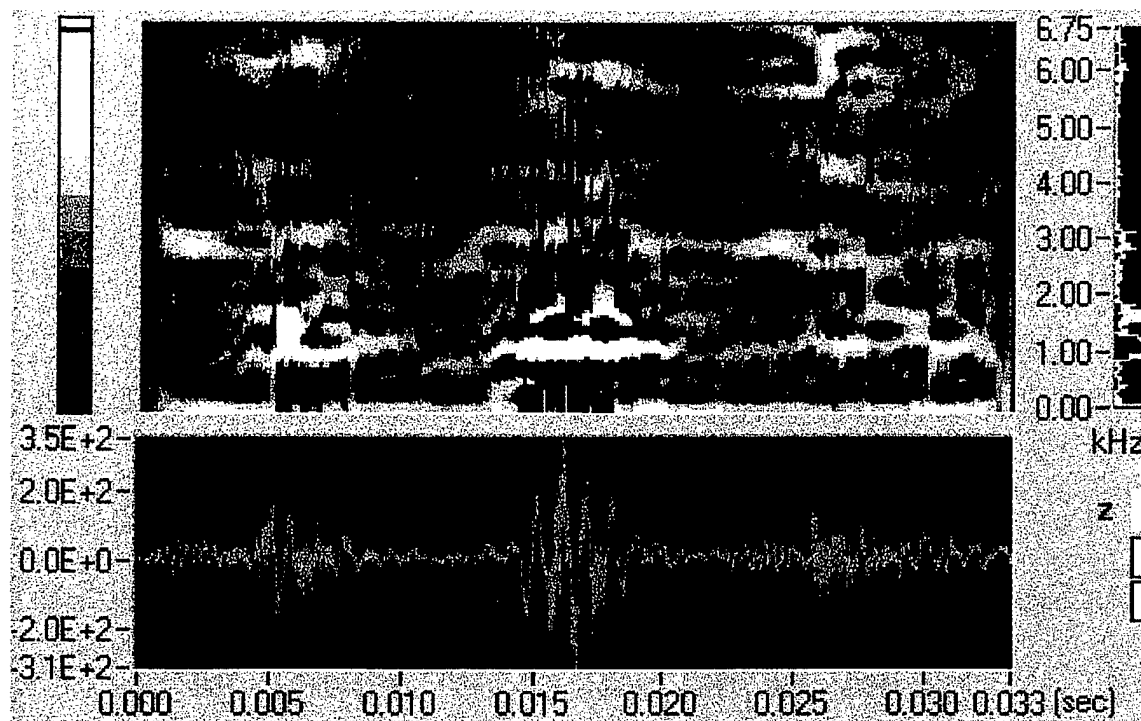
Figure 4.9 Cone-Shaped Distribution of the engine baseline vibration signal
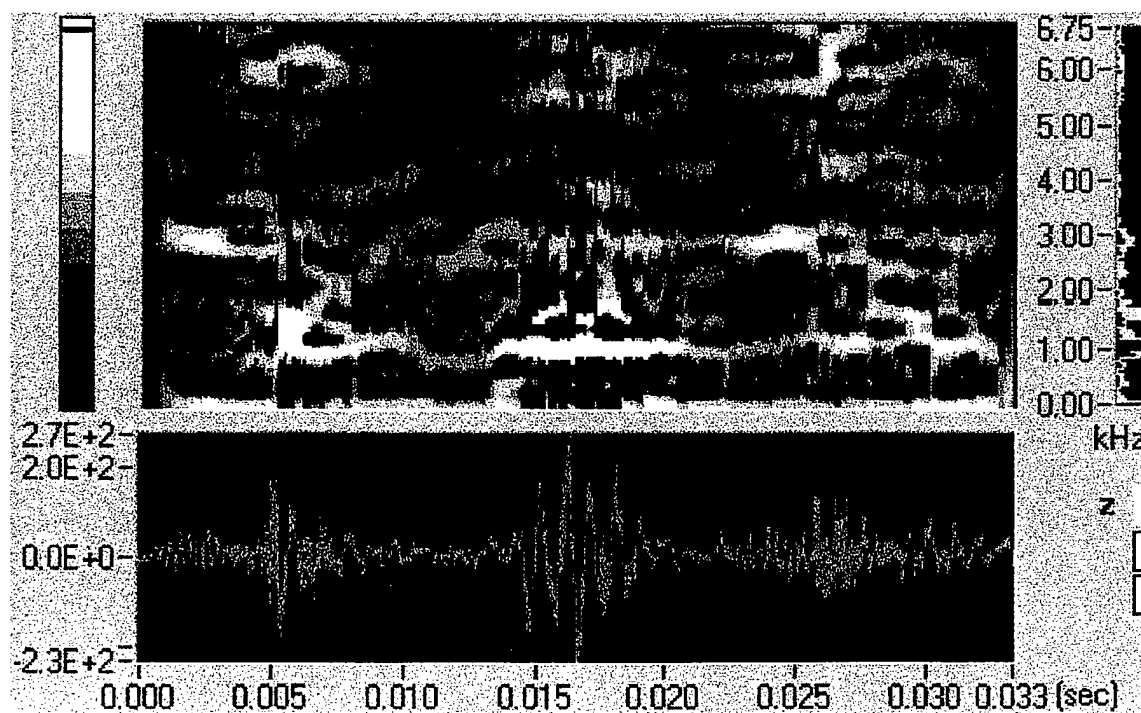
Figure 4.10 Cone-Shaped Distribution of the engine timing fault condition vibration signal

37

5. Choi-Williams Distribution (CWD)

Figure 4.11 shows the CWD of the baseline vibration signal. The timing fault condition vibration signal is shown in Figure 4.12. These CWD figures show excellent time and frequency resolution in the very narrow horizontal and vertical bands. However, the cross term interference and noise creates even more distortion than the CSD or Gabor Spectrogram. The CWD provides little or no useful information in determining the differences between the baseline and timing fault signals.

6. Adaptive Spectrogram (ASD)
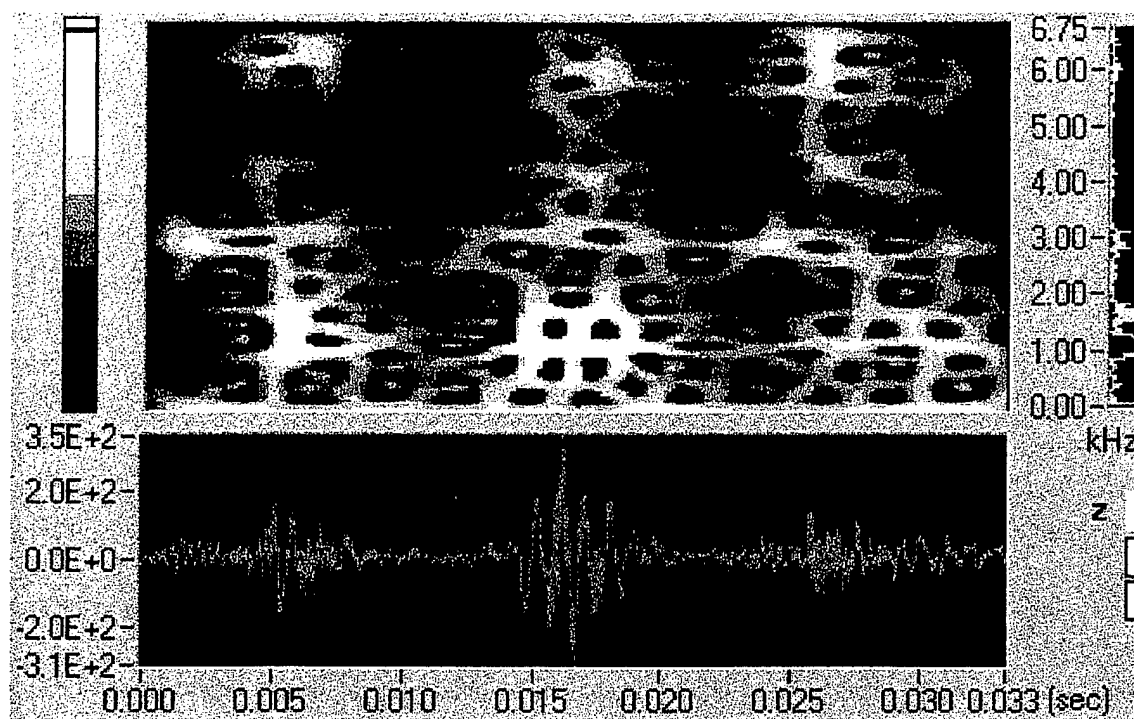
Figure 4.13 shows the ASD of the baseline vibration signal. The timing fault condition vibration signal is shown in Figure 4.14. The Joint Time Frequency Distribution shows localized energy peaks or islands with respect to time and frequency. As you would expect from examining the time domain vibration signal, the energy is concentrated in the time periods where each cylinder is firing. Since the vibration transducer is directly above the first cylinder, there are more islands displayed between 0.010-0.020 seconds. The magnitudes of these first cylinder islands are greater than those associated with the second and third cylinder firings. Some minor shifting or shape changes of the islands was found by comparing multiple data runs. Increasing the number of revolutions being sampled and averaged should increase the stability of the energy islands.

Now focus in on the period where the first cylinder is firing 0.010-0.020 seconds. There are several clear and distinct time-frequency peaks or islands at 0.5, 1.0, 1.5, 2.0, 3.0 and 6.0 khz. Exactly what each frequency island corresponds to in the engine is unknown and will require further study. The firing of the cylinder acts like a big hammer striking the engine. This impulse will undoubtedly cause many of the engine components to resonate at their individual natural frequencies. Some of the likely sources are the

38
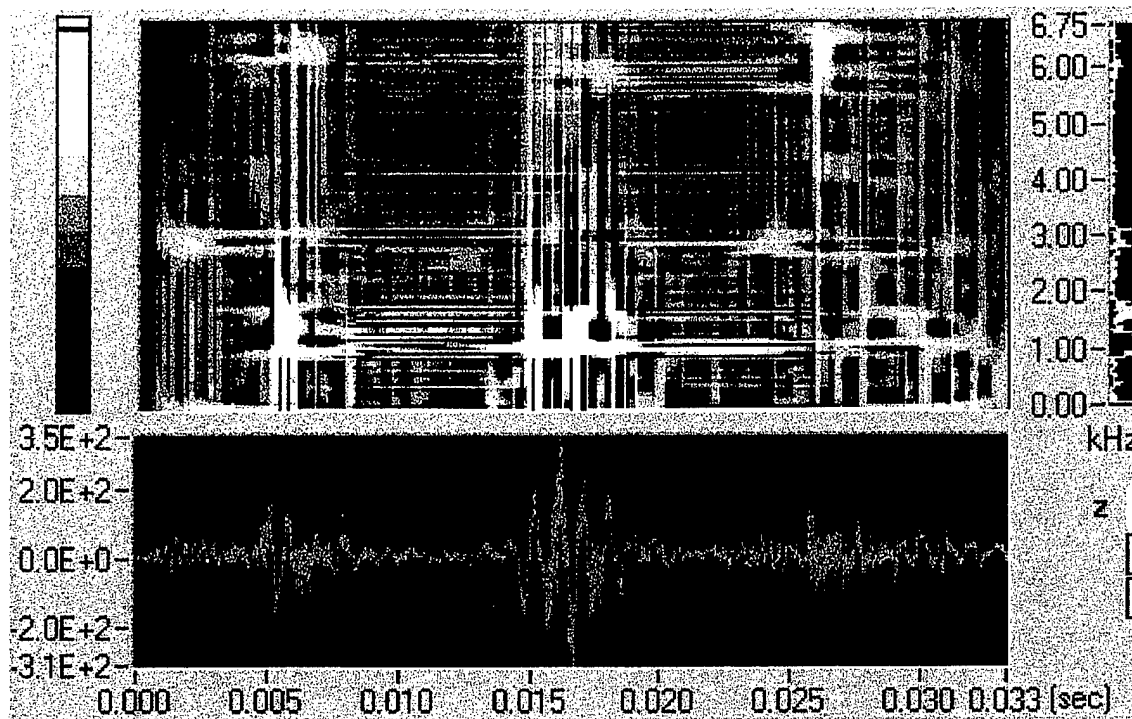
Figure 4.11 Choi-Williams Distribution of the engine baseline vibration signal
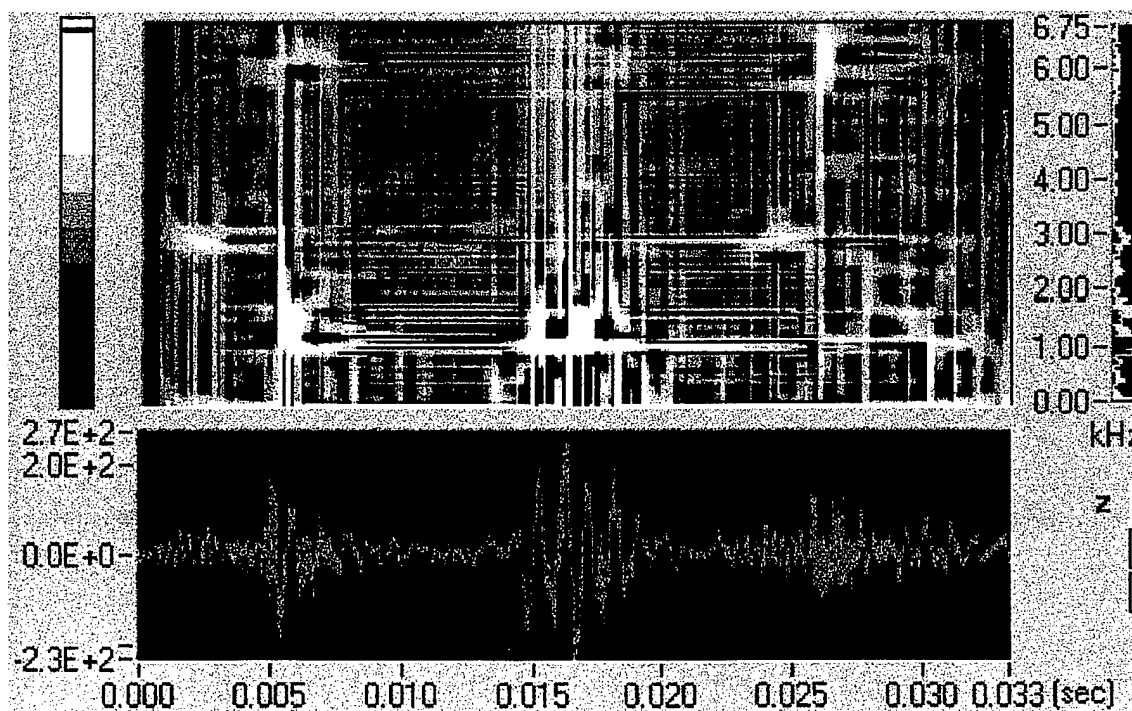
Figure 4.12 Choi-Williams Distribution of the engine timing fault condition vibration signal

39
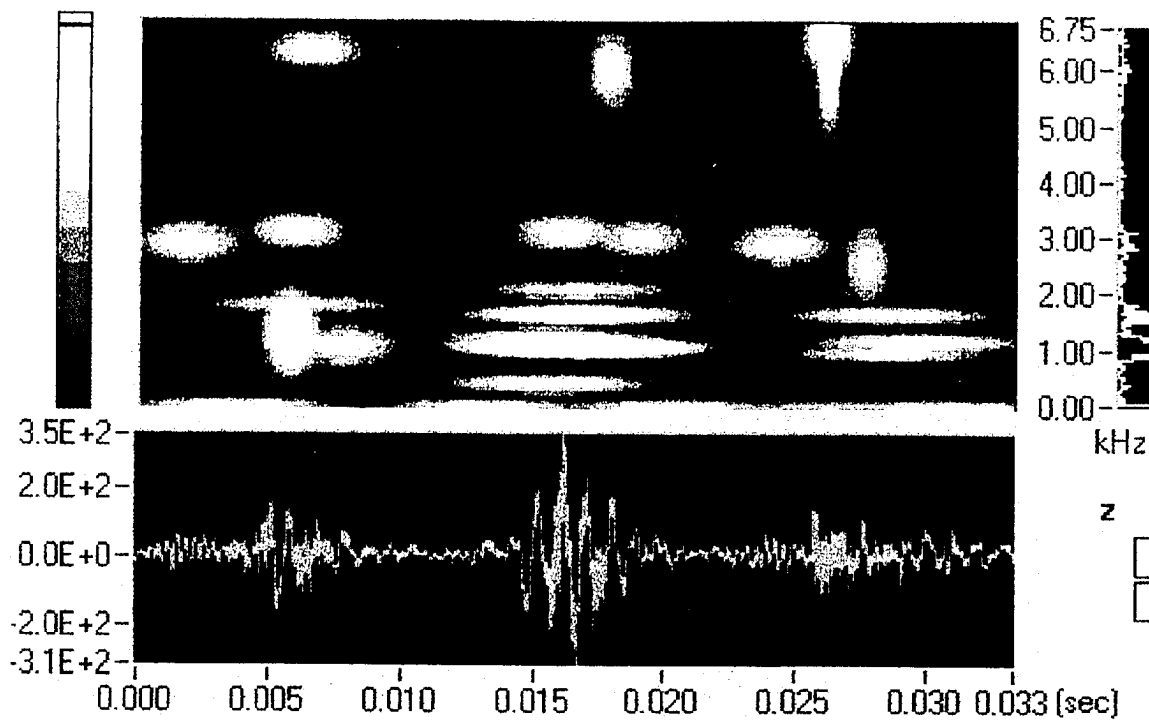
Figure 4.13 Adaptive Spectrogram of the engine baseline vibration signal
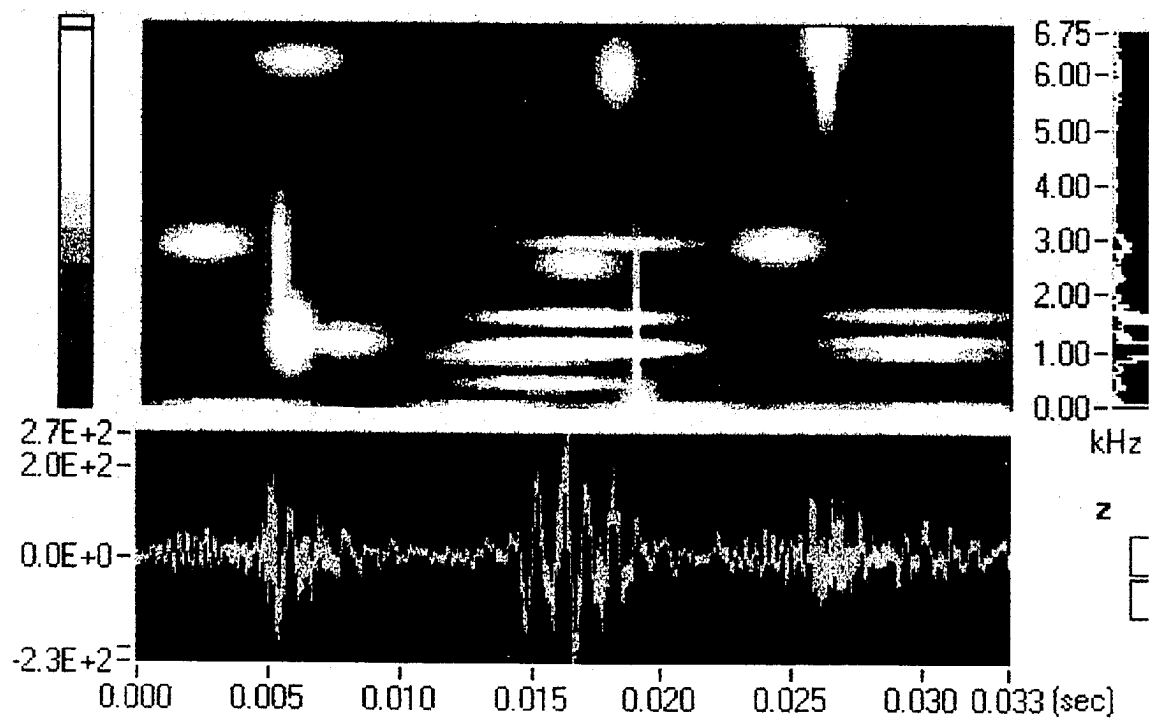
Figure 4.14 Adaptive Spectrogram of the engine timing fault condition vibration signal

40

block, piston, connecting rod and the cylinder head bolt. Another possible source could be the excitation of standing waves in the engine block.

Directly comparing the ASD of the baseline and fault condition signals, there is one feature which is clearly different. Figure 4.14 shows a broadband of energy at 0.018 seconds ranging from 0 to 3.5 khz. This feature does not occur in the baseline Figure 4.13. This broadband of energy could be the signature of a change in the combustion process due to the timing shift. This same broadband "scar" was found in all four of the data runs with the timing fault and did not appear in any of the four baseline data runs.

These Adaptive Spectrogram figures provide the best representation for the engine vibration signals. It provides fine resolution in both the time and frequency content. There is no cross term interference. The ability to reject noise enhances the readability of the joint distribution display.

V. CONCLUSIONS AND RECOMMENDATIONS

A Diesel engine test cell was completed and instrumented to make steady performance as well as time resolved measurements of cylinder pressure and head bolt acceleration. The facility is operational and capable of acting as a test bed for a wide variety of experimental investigations on Diesel engines.

A series of fuel injection timing faults were introduced into the engine to assess the ability of various methods to detect these faults. Based on experimental results the following conclusions were drawn:

1. It is possible to identify the retarded timing of the fuel injection by direct measurement of cylinder pressures.

2. The adaptive Joint Time Frequency Analysis was the most useful signal processing algorithm out of the six tried for interpreting the vibration time series signals from the engine head bolts. This was due to the large reduction in cross term interference and the relative simplicity of the topographical output.

3. There was a change in the adaptive JTFA map when the fuel injection timing fault was introduced. Cases with the mistiming had a vertical "scar" in frequency near the firing time of the cylinder in question. This repeatable change could be attributed to the dynamics of the timing. However, the physical mechanisms which create this phenomena and cause this characteristic signature are not understood.

Several additional areas may be helpful in clarifying this work as well as adding insight into creating and applying CBM methodologies to Diesel engines. In this regard, the following recommendations are submitted for future work.

1. Modal testing of various components and subassemblies to identify the natural frequencies and damping ratios. This should help identify the "islands" of the JTFA display.

2. Create dynamic models of the engine. Such models may be a useful tool in understanding the experimental data.

3. Time tag the data. The present data acquisition system takes phase locked data with the use of an encoder. For several reasons (measuring torsional speed variations, non-constant time spectral analysis, etc.) it would be useful to record the timing of the data acquisition events.

4. Identify other classes of faults, which are common to Diesel engines. Develop methods to quickly, cheaply and non-destructively introduce these faults for analysis and characterization.

Implementation of CBM shows tremendous potential savings in the maintenance of engines in the U.S. Navy. It will also provide considerable improvements in reliability and operational availability of the fleet.

LIST OF REFERENCES

1.   Marshall, B. R., "A Surface Navy Vibration Program Overview: Standardization and State-of-the-Art", Naval Engineers Journal, Vol. 100, May 1988, pp. 90-100.

2.   Update International, Inc., "A Practical Approach to Reciprocating Machinery Analysis".

3.   Ville, J., "Theorie et Applications de la Notion de Signal Analytique", Cables et Transmission, Vol. 2a, No. 1, pp. 61-74, 1948.

4.   Wigner, E., "On the Quantum Correction for Thermodynamic Equilibrium", Physics Review, Vol. 40, pp. 749-759, June 1932.

5.   Cohen, L., "Time-Frequency Distributions-A Review", Proceedings of the IEEE, Vol. 77, No. 7, pp. 941-981, July 1989.

6.   Qian, S. and Chen, D., "Signal Representation via Adaptive Normalized Gaussian Functions," Signal Processing, Vol. 36, No. 1, March 1994.

7.   "Labview Joint Time-Frequency Analysis Toolkit Reference Manual", National Instruments, Part No. 320544-01, March 1994.

8.   Rohrbaugh, R. and Cohen, L., "Time-Frequency Analysis of a Cam-Operated Pump", Life Extension of Aging Machines, pp. 349-361, Vibration Institute, Chicago, 1995.

9.   Zakrajesck, J., "A Review of Transmission Diagnostics Research at NASA Lewis Research Center", NASA Technical Memorandum 106746, December 1994.

10.   O'Conner, L., "Diagnosing Diesel Engines", Mechanical Engineering, pp. 44-50, March 1992.

11.   "Detroit Diesel Engines-Series 53 Service Manual", Part No. 6SE201, Revision December 1986.

APPENDIX A: ENGINE INSTALLATION PROBLEMS

1.   The first cylinder injector fuel control rack was stuck.

      Solution: Replaced all three injectors with rebuilt units.

2.   The oil supply line from the block to the governor assembly was hooked up to the air box drain port instead of an oil gallery port.

      Solution: Inspected and cleaned the oil out of the air box cavity. Reinstalled the oil line correctly.

3.   The thermostat was missing from the jacket water expansion housing.

      Solution: Removed the thermostat from the spare engine, tested and installed it.

4.   The front engine mounting plate was clamped directly to the dynamometer stand with no vibration mounts. The engine vibration was severe.

      Solution: Modified the mounting plate and installed 4 standard Navy Shock/Vibration Mounts.

5.   The fuel Pump installed on the engine was the wrong type. The rotation of the pump was incorrect, causing the relief valve to fail. Excess pressure in the pump caused fuel to blow past the seals and into the crankcase. The oil level increased by 3 inches within a very short run time.

      Solution: Replaced the fuel oil pump and changed the engine oil.

6.   The engine did not have an orifice flow restrictor in the return fuel oil line. It is required to maintain pressure in the fuel rack and injectors.

      Solution: Manufactured and installed the proper size orifice in the fuel oil line. Located at the compression fitting, for return oil, attached to the cylinder head.

7. The engine had significant oil leaks during the initial operational test. Leaks from the front vibration damper cover and the rear oil pan gasket continuously dripped. Solution: Installed 2 missing bolts from the front cover. Replaced one bolt which had the wrong thread type on the cover. Removed the oil pan and replaced the gasket which was torn and misaligned.

8. There was oil leaking from the exhaust pipe joints. Solution: Determined that it was leaking from the valve stem guides into the exhaust ports. The valve stem oil seals were missing. Ordered and installed new valve stem oil seals.

APPENDIX B: PERFORMANCE CURVES AND
MANUFACTURERS DATA

This appendix contains the manufacturers performance curves for the engine. These curves give information about the power output, torque and fuel consumption of the engine with respect to engine speed. Also included are specifications for the engine and various components.

General Data

Model	5033-5001
Number of Cylinders	3
Bore and Stroke-in(mm)	3.875x4.5(98x114)
Displacement-in³(L)	159(2.61)
Compression Ratio	21.0:1
Piston Speed-ft/min(m/min)	2100(640)
Valves Per Cylinder	
Intake	NOT APPLICABLE
Exhaust	4
Combustion System	DIRECT INJECTION
Engine Type	INLINE-2 CYCLE
Aspiration	NATURAL

Configuration

Turbocharger	NONE
Charge Air Cooling System	NOT APPLICABLE
Blower Type	STANDARD
Blower Drive Ratio	2.49:1
Low Idle Speed-r/min	550
High Idle Speed-r/min	2965
Thrust Bearing Load Limit	
Continuous-lbf(N)	400(1779)
Intermittent-lbf(N)	1200(5338)
Engine Crankcase Vent System	OPEN
Maximum Pressure-in H_2O(kPa)	3(0.75)

Physical Data

Size	
Length-in(mm)	33(838)
Width-in(mm)	27(686)
Height-in(mm)	35(889)
Weight,dry-lb(kg)	965(438)
Center of Gravity Distance	
From R.F.O.B. (x axis)-in(mm)	7.5(190)
Above Crankshaft (y axis)-in(mm)	9.16(233)
Right of Crankshaft (z axis)-in(mm)	1.79(45.5)
Installation Drawing	5124661
Maximum Allowable Static Bending Moment at Rear Face of FW Hsg-lbf ft(N m)	0

Fuel System

Fuel Injector/Timing	N45/1.460
Fuel Injection Pump/Timing	NOT APPLICABLE
Fuel Consumption-lb/hr(kg/hr)	40.2(18.2)
Fuel Consumption-gal/hr(L/hr)	5.8(21.9)
Fuel Spill Rate-lb/hr(kg/hr)	349.5(158.5)
Fuel Spill Rate-gal/hr(L/hr)	50.0(189.3)
Total Fuel Flow-lb/hr(kg/hr)	389.7(177)
Total Fuel Flow-gal/hr(L/hr)	55.8(211)
Maximum Allowable Fuel Pump Suction	
Clean System-in Hg(kPa)	6(20)
Dirty System-in Hg(kPa)	12(41)
Fuel Filter Micron Size	
Primary - Micron	30
Secondary - Micron	10

Lubrication System

Oil Pressure	
Rated Speed-lbf/in²(kPa)	40(276)
Low Idle-lbf/in²(kPa)	5(34)
In Pan Oil Temperature-°F(°C)	200-250(93-121)
Oil Flow-gal/min(L/min)	21(79)
Oil Pan Capacity	
High-qt(L)	10.5(9.9)
Low-qt(L)	7.5(7.1)
Total Engine Oil Capacity with filters-qt(L)	12.5(11.8)
Bypass Oil Filter Orifice-in(mm)	0.062(1.57)
Engine Angularity Limits	
Front up - degrees	20
Front down - degrees	30
Side tilt - degrees	NOT AVAILABLE

Emission Data

CO-gm/hr	NOT AVAILABLE
HC-gm/hr	NOT AVAILABLE
NO_x-gm/hr	NOT AVAILABLE
SO_x-gm/hr	NOT AVAILABLE
Smoke	NOT AVAILABLE
Rated Speed - Bosch Number	NOT AVAILABLE
Peak Torque Speed - Bosch Number	NOT AVAILABLE
Noise - dB(A) @ 1m	NOT AVAILABLE
Certification Approval	NOT APPLICABLE

Cooling System

Engine Heat Rejection-Btu/min(kW)	3036(53)
Engine Radiated Heat-Btu/min(kW)	960(17)
Coolant Flow-gal/min(L/min)	38(144)
Thermostat	
Start to Open-°F(°C)	170(77)
Fully Open-°F(°C)	187(86)
Maximum Water Pump Inlet Restriction-in Hg(kPa)	3(10)
Engine Coolant Capacity-qt(L)	8(7.6)
Minimum Pressure Cap-lbf/in²(kPa)	7(48)
Maximum Coolant Pressure-(Exclusive of Pressure Cap)-lbf/in²(kPa)	NOT AVAILABLE
Maximum Top Tank Temperature-°F(°C)	210(99)
Minimum Top Tank Temperature-°F(°C)	170(77)
Minimum Coolant Fill Rate-gal/min(L/min)	3(11)
Cooling Index	
Minimum Air to Boil-°F(°C)	NOT APPLICABLE
Maximum Air to Water Diff.-°F(°C)	95(53)
Ram Air Flow - Mile/hr(km/hr)	NOT APPLICABLE
Deaeration-Air Injection Capacity-ft³/min(m³/min)	0.3(0.008)
Drawdown - Minimum Requirement (or 10% of Cooling System Capacity-Whichever is Larger)-qt(L)	4(3.8)

Air System

Maximum Allowable Temperature Rise (Ambient Air to Engine Inlet)-°F(°C)	30(17)
Air Intake Restriction Maximum Limit	
Dirty Air Cleaner-in H_2O(kPa)	25(6)
Clean Air Cleaner-in H_2O(kPa)	16(4)
Engine Air Flow - ft³/min(m³/min)	275(7.8)
Engine Air Box/Manifold Pressure-in Hg(kPa)	7.8(26)
Recommended Intake Pipe Dia.-in(mm)	3.0(76)

Exhaust System

Exhaust Flow-ft³/min(m³/min)	660(18.7)
Exhaust Temperature-°F(°C)	825(440)
Maximum Allowable Back Pressure-in Hg(kPa)	4(13.5)
Recommended Exhaust Pipe Dia.	
Single-in(mm)	3.0(76)
Dual-in(mm)	NOT APPLICABLE
Exhaust Brake Max. Allowable Back Pressure-in Hg(kPa)	NOT AVAILABLE

Electrical System

Recommended Battery Capacity(CCA @ 0°F)	
12 Volt System	
Above 32°F(0°C)-A	475
Below 32°F(0°C)-A	625
24 Volt System	
Above 32°F(0°C)-A	475
Below 32°F(0°C)-A	625
Maximum Allowable Resistance of Starting Circuit	
12 volt system - ohm	0.0012
24 volt system - ohm	0.002

Performance Data

Power Output-bhp(kW)	92(68.6)
Full Load Speed-r/min	2800
Peak Torque-lb ft(N m)	198(268)
Peak Torque Speed-r/min	1500
BMEP-lbf/in²(kPa)	83(572)
Friction Power	
Rated Speed-fhp(kW)	42(31)
Peak Torque Speed-fhp(kW)	15(11)
Altitude Capability-ft(m)	8000(2438)
Torque Available at 800 r/min-lb ft (N m)	NOT AVAILABLE

Engine Speed r/min	Power bhp(kW)	Torque lb ft(N m)	BSFC lb/bhp hr (g/kW hr)
2800	92(69)	173(235)	.437(266)
2500	87(65)	184(249)	.426(259)
2200	80(60)	192(260)	.426(259)
1800	69(51)	198(268)	.433(263)
1500	57(43)	196(461)	.457(278)

50

MECHANICAL DATA FOR 3 & 4-53N ENGINES

MAIN BEARINGS
Type..Precision Half Shells - 2 per Journal

Journal Diameter ....3.0 in.(76.2 mm)
Length ....1.18 in.(30.0 mm)
Projected Area/Bearing ..3.54 in^2(2284 mm^2)
Material ....Steel Backed Copper Lead

CRANK PIN BEARINGS
Type....................Precision Half Shell

Number............................1 Pair/cyl
Journal Diameter..........2.50 in.(63.5 mm)
Length....................1.31 in.(33.3 mm)
Projected Area/Bearing...3.28 in^2(2113 mm^2)
Material...........Steel Backed Copper Lead

CAMSHAFT BEARING - END
Journal Diameter..........2.18 in.(55.4 mm)
Length....................1.50 in.(38.1 mm)
Materials...............SAE 799 Steel Backed

CAMSHAFT BEARING - INTERMEDIATE
Journal Diameter..........2.18 in.(55.4 mm)
Length....................1.50 in.(38.1 mm)
Materials...............SAE 799 Steel Backed

PISTON PIN BUSHING
Material..Bronze with SAE 19 Overlay, Steel
Backed

PISTON
Type and Material......Trunk-Malleable Iron
Cooling..................Pressure Oil Spray

PISTON RINGS - COMPRESSION
Type
  Top Ring.........Chrome Faced Rectangular
  Remaining 2......Chrome Faced Rectangular

PISTON RINGS - OIL
Type...........Double Scraper with Expander
Number per Piston.....................2 Sets
Location....................Bottom of Skirt

PISTON PIN
Type...............................Solid

CONNECTING ROD
Type .... Forged I Section
Material ....Forged Steel

CRANKSHAFT
Material............Forged Steel(SAE1548)
Type of Balance....................Dynamic
Heat Treat.............Induction Hardened

CAMSHAFT
Material....................Forged Steel
Location..........................In Block
Drive................................Gear
Type of Cam........................Ground

EXHAUST VALVE
Type................................Poppet
Arrangement.................Overhead Valve
Number/Cylinder.........................4
Operating Mechanism..Mechanical Rocker Arm
Type of Lifter.....................Roller
Valve Spring
  Number/Valve.................1 Per Valve
Valve Seat Insert
  Material....................Steel Alloy

CYLINDER BLOCK
Type...............................One Piece
Material....................Cast Iron Alloy

LINERS
Type...............................Wet Liner
Material.....................Gray Cast Iron
Ports
  Type...............................Oval
  Number...............................18

CYLINDER HEAD
Type...........................Slab 4 Valve
Material.........................Cast Iron

ENGINE PERFORMANCE CURVE

Detroit Diesel Allison

RATING: RATED BRAKE POWER

APPLICATION: INDUSTRIAL

MODEL: 3-53N
92 bhp @ 2800 r/min
198 lb·ft @ 1800 r/min
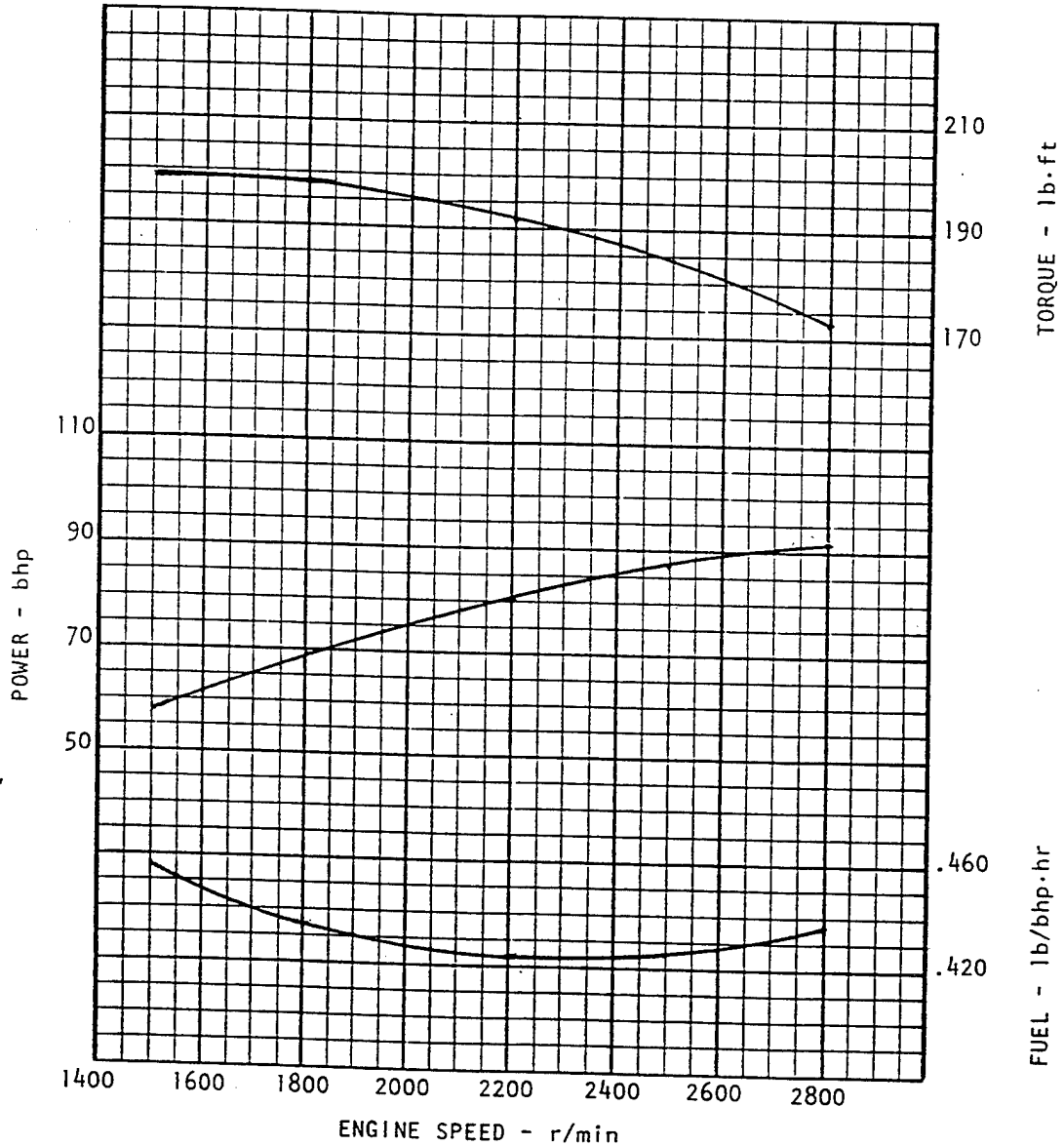
UNCONTROLLED

AIR INTAKE RESTRICTION - in. H₂O (kPa) . . . 10 (2.5)
EXHAUST BACK PRESSURE - in. H₂O (kPa). . . . 15 (3.7)

- POWER OUTPUT GUARANTEED WITHIN 5% AT SAE J1349 CONDITIONS:
77°F (25°C) AIR INLET TEMPERATURE; 29.31 In. Hg (99kPa) DRY BAROMETER;
100°F (39°C) FUEL INLET TEMPERATURE (.853 SPECIFIC GRAVITY AT 60°F).
- CONVERSION FACTORS: POWER: kW = bhp x 0.746
                        FUEL: kg/kW·hr = lb/bhp·hr x 0.608
                        TORQUE: N·m = lb·ft x 1.356
- VALUES DERIVED ARE FROM CURRENTLY AVAILABLE DATA AND SUBJECT TO
CHANGE WITHOUT NOTICE.

CERTIFIED BY:

Mark J. Kuhn

STAFF ENGINEER

CURVE NO.
E4-5031-52-3
DATE: 11-26-63
REV./DATE: 2/8-3-87
SHT. 1 OF 4

52

ENGINE PERFORMANCE CURVE

DETROIT DIESEL ALLISON

ENGINE DESCRIPTION: 3-53N
APPLICATION: INDUSTRIAL
INJECTOR: N-45   1.460 TIMING
TURBOCHARGER: NONE

LINES OF CONSTANT FUEL CONSUMPTION LB/BHP-HR

BSFC
0.430
0.440
0.460
0.480
0.500
0.520
0.540
0.560
0.580

BRAKE HORSEPOWER

ENGINE SPEED (RPM)
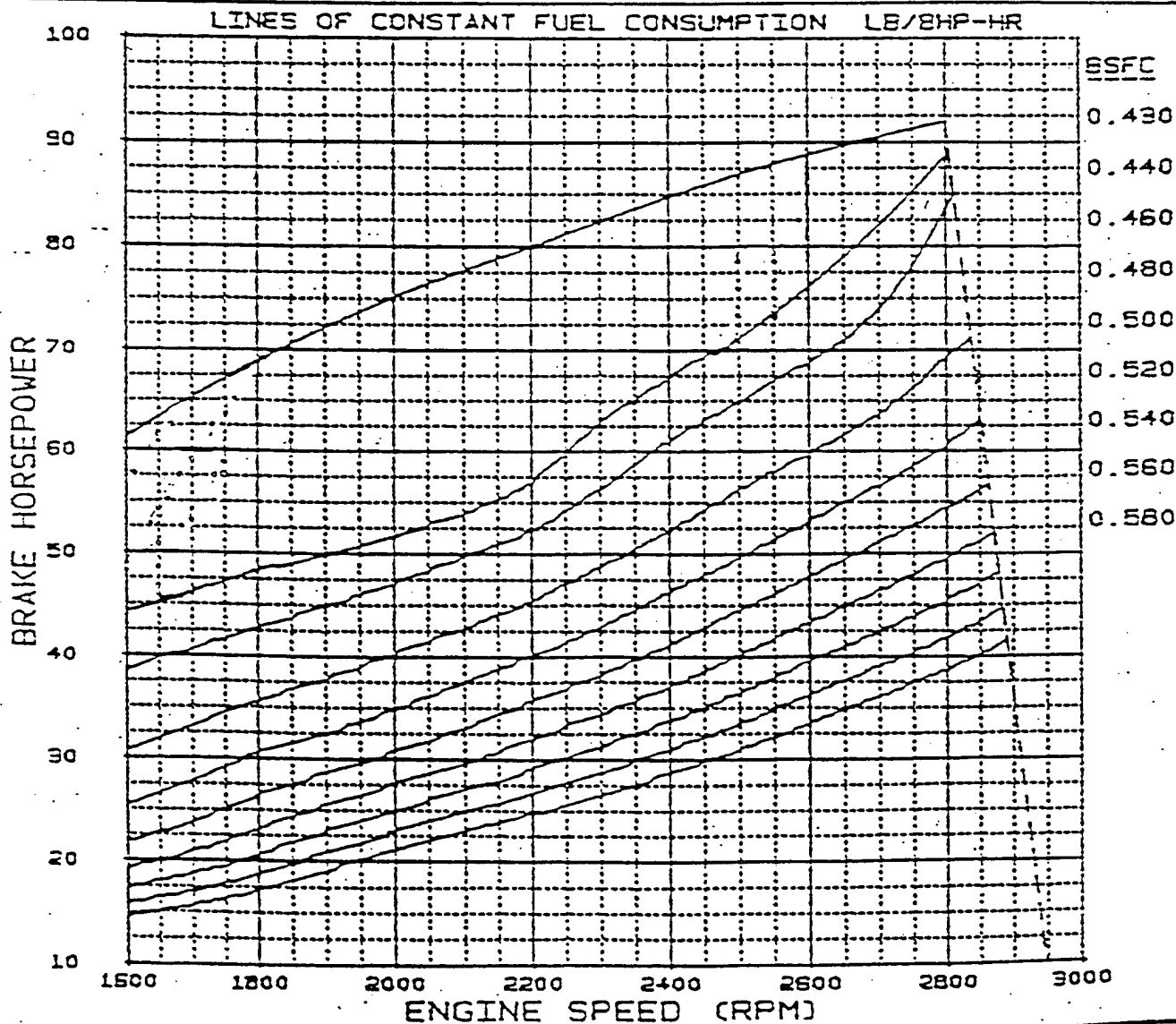
STANDARD CONDITIONS: (SAE J1349 AMBIENT)
77 F (25.0 C) AIR TEMPERATURE
29.32 IN HG (99.0 KPA) BAROMETER (DRY)
100 F (37.8 C) FUEL INLET TEMPERATURE
0.838 FUEL SPECIFIC GRAVITY (0.853 /60 F)
VALUES ARE DERIVED FROM CURRENTLY AVAILABLE
DATA AND ARE SUBJECT TO CHANGE WITHOUT NOTICE.

CURVE NO:
E4-5031-52-3
DATE: 11-26-63
FILE: D03N45

REVISION: 2/8-3-87
SHT. 3 OF 4.

53

ENGINE FRICTION HORSEPOWER

ENGINE FRICTION HORSEPOWER
SERIES 53N ENGINES

ENGINE SPEED - RPM

3-53N
4-53N
6V-53N
8V-53N
12V-53N

E4P-5000-52-1

E 2236

54
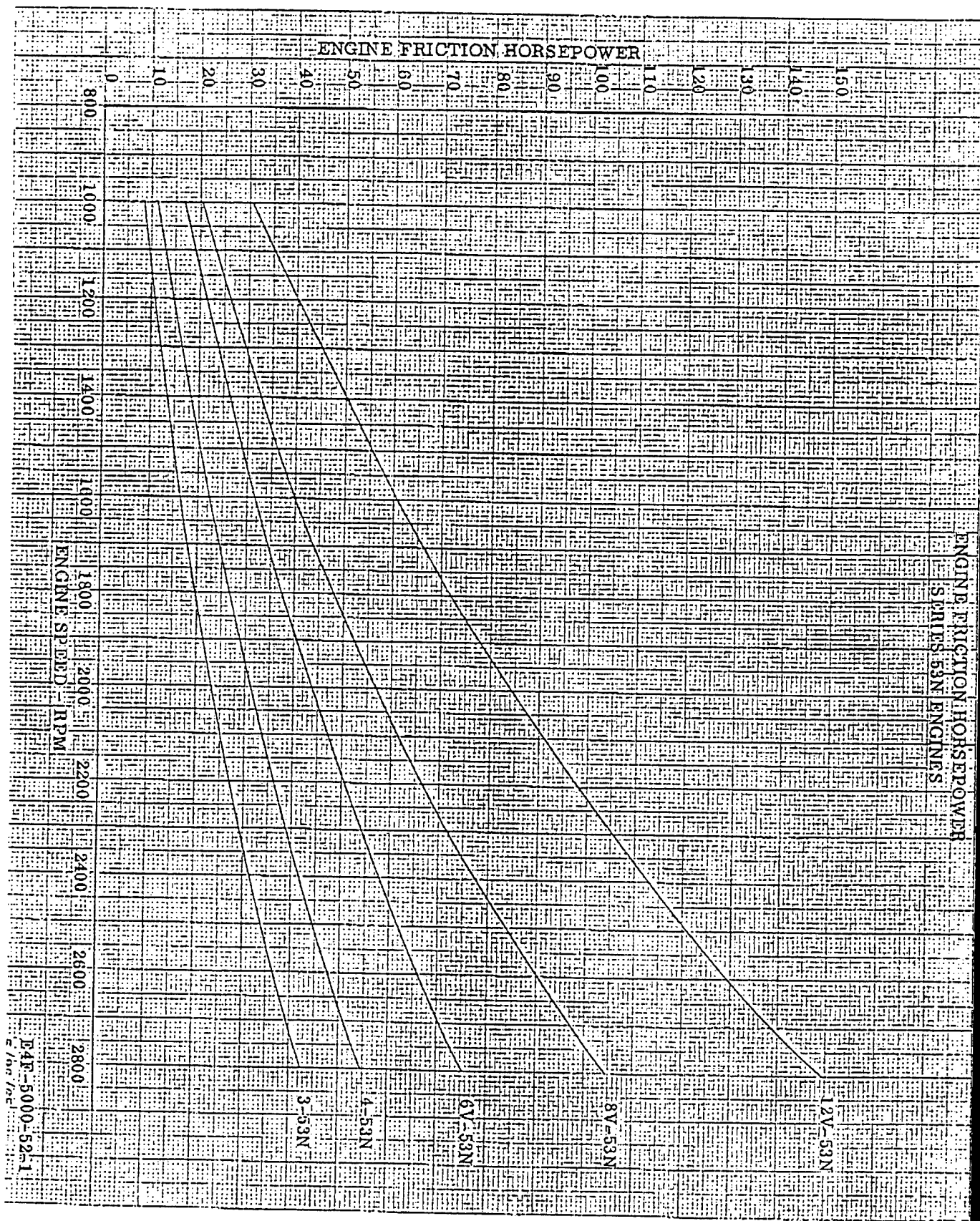
APPENDIX C: DETAILED OPERATING PROCEDURES FOR THE DIESEL ENGINE

SYSTEM ALIGNMENT AND PREPARATION

1. Turn power on for the following equipment and allow 20 minutes of warm up time.

    Kistler Charge Amplifiers
    PCB Conditioning Amplifiers
    Krohn-Hite Low Pass Filter
    H-P Oscilloscope
    ECA Sensor Interface
    Dynamometer Control Computer
    ECA Control Computer
    Dynamometer Console

2. Align the dynamometer water and fuel system.
    Ensure the water supply and return valves to the gas turbine cell are closed or the water will overflow in the gas turbine cell.

3. Ensure that the Diesel air flapper valve is open and latched.

4. Open the cell vent duct shutters.

5. Ensure the cell ventilation is turned on.

6. Start the dynamometer water system heat exchanger fan.

7. Start the water return pump.

8. Start the water supply pump.

9. Open the power absorber boost cutout valve.

10. Adjust the water return throttle valve to obtain a steady water level in the discharge tank.

11. Close the engine cell doors.

12. Start the main fuel pump.

STARTING AND OPERATING THE ENGINE

1. Adjust the torque display to zero.

2. Check the initial setup of the console:
    Throttle control - Manual
    Load control - Manual
    Load Set point - 8 on the voltmeter scale ~ 40%
    Ignition switch - ON   (power for the local gages)

3. Start the dynamometer fuel pump.

4. Press and hold the starter button until the engine starts about 2-5 seconds.   Watch for the oil pressure to rise on the console gage.

5. Adjust the throttle servo rpm control and the load torque control to match the engine operating conditions.

6. Watch the servo motor on the engine stand while switching the throttle control to servo. Ensure that the throttle is responding correctly before continuing.

7. Switch the load control to servo.

8. Increase the rpm setpoint to 1300 rpm and the torque setpoint to 120 ft-lbs. Allow the engine to warm up.

9. After the jacket water out temperature reaches 180° F, adjust the speed and torque setpoints to the desired test conditions.

SECURING THE ENGINE

1. When finished operating decrease the speed and torque setpoints to idle conditions. Switch the torque control to manual and then the throttle control to manual.

2. Allow the engine to cool down and then shut it off by pulling the black T-handle.

3. Turn off the dynamometer fuel pump from the console toggle switch.

4. Turn off the main fuel pump and the cooling fan from the remote control box by the door.

5. Turn off the dynamometer water supply pump and then the return pump.

6. Close the power absorber boost cutout valve.

7. Close the water supply and return valves in the cell.

8. After the cell has cooled down, close the cell vent duct shutters.

9. Secure power to all computers and data collection hardware.

APPENDIX D: DATA COLLECTION INSTRUCTIONS AND SAMPLE DATA FILE

DATA COLLECTION WITH THE ECA

1.   On the ECA computer, select Data Taking and Statistics.

2.   Select the default setup file DD353.SET.

3.   Switch the Kistler Charge Amplifier to the Operate mode.

4.   Select Graph Monitor <G> to observe the engine signals.

5.   Select Data Taking to sample and store the data.

6.   Select Data Averaging to store the averaged cycle data to the hard drive.
    note: All data files are stored in directory C:\dat\base.

7.   The standard file naming format is:

Letter for grouping data runs			Accelerometer ID Number
		A1818C11.DAT	
Engine Speed x100 rpm			Standard File Extention for Averaged Data
Engine Torque x10 ft-lbs			Data Run Number for Multiple Runs
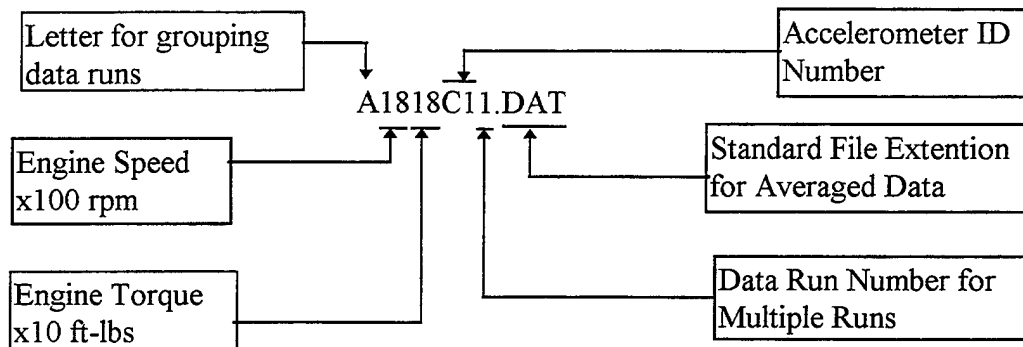
8.   To prepare the file for loading into the JTFA Toolkit, edit it in a text editor such as Windows Notepad. Delete the header and footer information so that only the data point values remain. Save the file with a new extension(filename.ASK) as an test data file.

9.   Load the file into the JTFA Toolkit using instructions in the reference manual [Ref. 7].

SAMPLE DATA FILE

2,.1,3 ←———————————— [Header Information]

-14.06323 ←┐
-14.88582
-15.69483
-14.12199
-9.98774
-6.368441
-3.516525
   "
   "
   "   [Data Point Magnitudes
   "   Total of 3600 points]
21.22029
18.52735
17.10666
16.12848
10.90861
1.959038
-3.685864
-6.776357
-10.00841
-12.49026 ←┘
3.88,4.5,8.8,0,21,90,85 ←┐
1,-14.0632290590147,310.7778,1,1806.355,0,1,69
11-25-1995,00:02:47,,C,D
0,"Vib1y","g",3   [Footer Information]
-30,0,"N",1,100,5.715,"I3-53.2D","",""
" "
" "
" "
" " ←┘

60
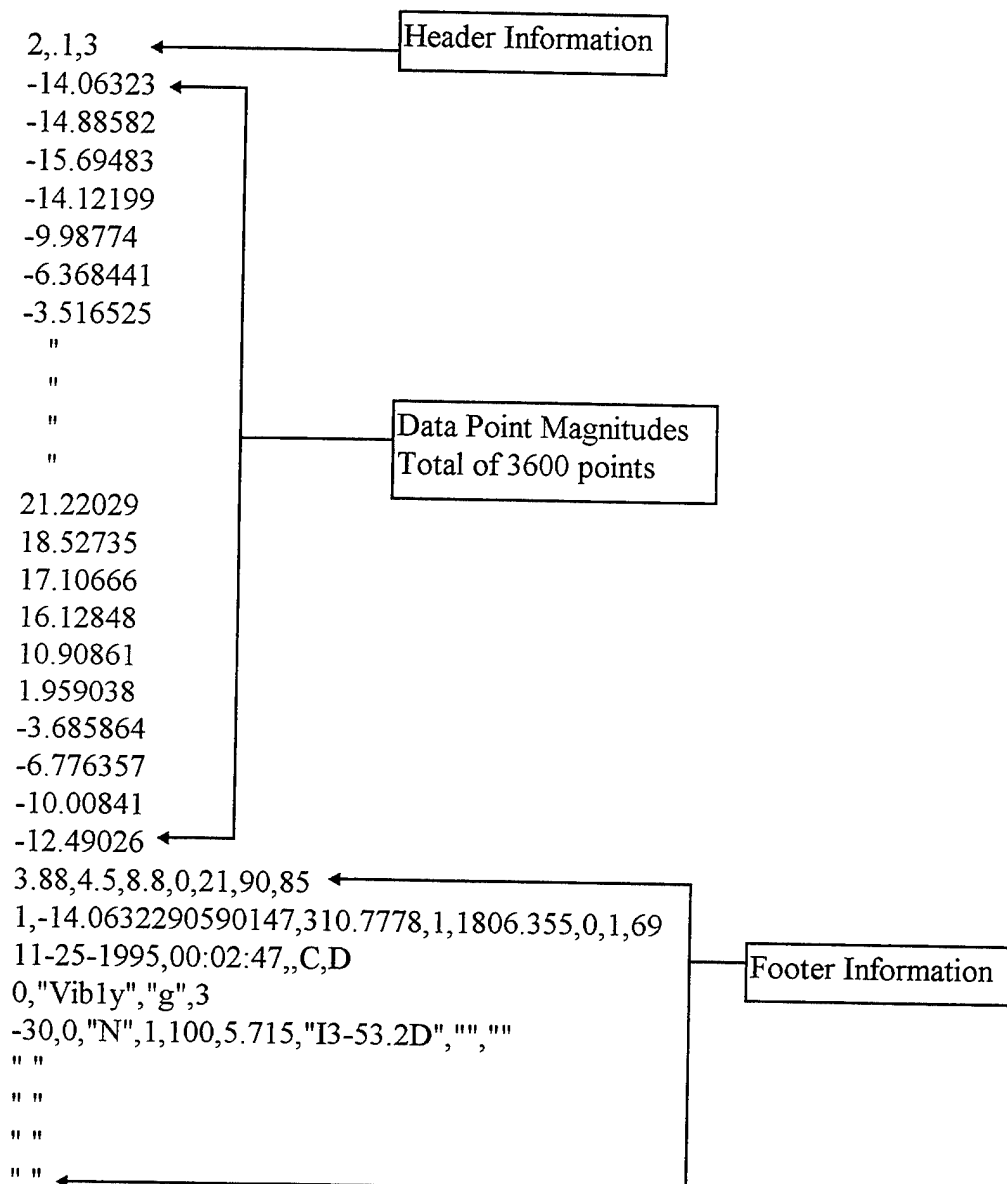
INITIAL DISTRIBUTION LIST

		No. Copies
1.	Defense Technical Information Center	2

8725 John J. Kingman Road, Ste. 0944
Ft. Belvoir, VA 22060-6218

2. Dudley KnoxLibrary 2
Naval Postgraduate School
411 Dyer Rd.
Monterey, CA 93943-5101

3. Department Chairman, Code ME 1
Department of Mechanical Engineering
Naval Postgraduate School
Monterey, CA 93943-5000

4. Professor Knox T. Millsaps Jr., Code ME/MI 4
Department of Mechanical Engineering
Naval Postgraduate School
Monterey, CA 93943-5000

5. Curricular Officer, Code 34...1
Department of Mechanical Engineering
Naval Postgraduate School
Monterey, CA 93943-5100

6. LT Robert Armstrong...2
5777A Erne Ave
Ewa Beach, HI 96706

7. Mr. John Moschopoulos 1
Naval Sea Systems Command (SEA 03J)
NC-4
2531 Jefferson Davis Highway
Arlington, VA 22242-5160

8.	Mr. William Hamilton 1
	Naval Sea Systems Command (SEA 03X)
	NC-4
	2531 Jefferson Davis Highway
	Arlington, VA 22242-5160

9.	Bentley Nevada Corporation 1
	Mr. Don Bentley
	P.O. Box 157
	Minden, NV 89423